

A practical phase field method for an elliptic surface PDE

Article (Accepted Version)

Barrett, John W, Deckelnick, Klaus and Styles, Vanessa (2020) A practical phase field method for an elliptic surface PDE. IMA Journal of Numerical Analysis. ISSN 0272-4979

This version is available from Sussex Research Online: <http://sro.sussex.ac.uk/id/eprint/91584/>

This document is made available in accordance with publisher policies and may differ from the published version or from the version of record. If you wish to cite this item you are advised to consult the publisher's version. Please see the URL above for details on accessing the published version.

Copyright and reuse:

Sussex Research Online is a digital repository of the research output of the University.

Copyright and all moral rights to the version of the paper presented here belong to the individual author(s) and/or other copyright owners. To the extent reasonable and practicable, the material made available in SRO has been checked for eligibility before being made available.

Copies of full text items generally can be reproduced, displayed or performed and given to third parties in any format or medium for personal research or study, educational, or not-for-profit purposes without prior permission or charge, provided that the authors, title and full bibliographic details are credited, a hyperlink and/or URL is given for the original metadata page and the content is not changed in any way.

A Practical Phase Field Method for an Elliptic Surface PDE

John W. Barrett[†]

Klaus Deckelnick[‡]

Vanessa Styles[§]

Abstract

We consider a diffuse interface approach for solving an elliptic PDE on a given closed hypersurface. The method is based on a (bulk) finite element scheme employing numerical quadrature for the phase field function and hence is very easy to implement compared to other approaches. We estimate the error in natural norms in terms of the spatial grid size, the interface width and the order of the underlying quadrature rule. Numerical test calculations are presented which confirm the form of the error bounds.

Key words. elliptic surface PDE, diffuse interface, finite element method, error analysis

AMS subject classifications. 35R01, 65M60, 65M15

1 Introduction

Let $\Gamma \subset \mathbb{R}^{n+1}$ ($n = 1, 2$) be a closed hypersurface. In this paper we are concerned with a phase field approach for the numerical solution of the PDE

$$-\Delta_{\Gamma}u + u = f \quad \text{on } \Gamma \tag{1.1}$$

and more general elliptic PDEs on surfaces. Here, Δ_{Γ} denotes the Laplace–Beltrami operator and f is a given function on Γ . Apart from being of interest in their own right, elliptic surface PDEs may arise as subproblems in the time discretization of parabolic surface PDEs as well as in systems involving a coupling to a bulk PDE (see e.g. [18]).

A major issue in the design and analysis of numerical methods for (1.1) lies in the fact that the simultaneous approximation of the PDE and of the surface Γ is required. Let us briefly review the various computational approaches that have been suggested in the literature. Further references can be found in the nice review articles [15] and [3].

In his seminal paper [14], Dziuk proposes a method that employs continuous, piecewise linear finite elements on a regular polyhedral approximation of Γ . For his scheme he obtains an $O(h)$ error bound in $H^1(\Gamma)$ and an $O(h^2)$ bound in $L^2(\Gamma)$. This approach has been extended to higher order FEM spaces and higher order polynomial approximations of Γ by Demlow in [11], while an adaptive version of the method can be found in [12]. However, the construction of

[†]John passed away on 30 June 2019. We dedicate this article to his memory.

[‡]Institut für Analysis und Numerik, Otto-von-Guericke-Universität Magdeburg, 39106 Magdeburg, Germany

[§]Department of Mathematics, University of Sussex, Brighton, BN1 9RF, UK

a regular polynomial approximation may be difficult in practice, in particular if the surface is given implicitly in terms of a level set function. The trace finite element method, proposed by Olshanskii, Reusken and Grande in [25], is based on a background mesh which induces an unfitted approximation Γ_h of Γ and employs traces of bulk finite element functions. Even though Γ_h is in general not regular, an $O(h)$ error estimate in $H^1(\Gamma_h)$ and an $O(h^2)$ bound in $L^2(\Gamma_h)$ for piecewise linear finite elements are obtained. Further developments and variants of this trace method (also called cut finite element method) can be found in [24], [9, Section 3], [28], [20], [13], [5] and [6].

In the case of a level set representation of Γ there is a class of methods that is based on extending the PDE (1.1) to an open neighborhood of Γ . Using earlier ideas of [2], Burger considers in [4, Section 2] an extension with the property that (1.1) is satisfied simultaneously on all neighboring level surfaces. This approach gives rise to a weakly elliptic bulk PDE, which is degenerate in the direction normal to the level surfaces and which can be solved numerically with the help of standard bulk finite elements. Error estimates have been derived in [4, Theorem 6], while [8] considers the problem in a narrow band of width h around Γ and provides an $O(h)$ bound in $H^1(\Gamma)$. In both cases the corresponding error analysis is complicated by the degeneracy of the extended PDE; an extended PDE, which is uniformly elliptic, has been proposed in [7] and [26] and involves the mean curvature of Γ . A different method which leads to a uniformly elliptic bulk PDE, is obtained by considering the equation which is satisfied by a natural extension of the solution of the surface PDE. If Γ is given implicitly in terms of the signed distance function this extension is the function which is constant in normal direction, and one is led to the closest point method, see [23] for the parabolic case. In the case of a general level set function the corresponding PDE has been derived in [9], where unfitted sharp and narrow band finite element methods have been proposed, and $O(h)$ and $O(h^2)$ error estimates in H^1 and L^2 respectively, have been shown.

Note that for schemes that are based on an implicit representation of the types described above computations are typically carried out on sets of the form $\Gamma_h = \{x \in \Omega \mid (I_h\phi)(x) = 0\}$ or $D_h = \{x \in \Omega \mid |(I_h\phi)(x)| < \gamma h\}$, where ϕ is the level set function describing Γ , and $I_h\phi$ is the linear interpolation of ϕ . These sets are unfitted to the underlying triangulation and hence may cut arbitrarily through a bulk element, see e.g. Fig. 2.1 in [25] or Fig. 1 in [9]. Locating these cuts and integrating over the discrete surface or partial elements is in general cumbersome. A way to circumvent these difficulties is offered by the use of a diffuse interface method. The starting point of this approach is again an extension of the surface PDE to a neighborhood of Γ , which is then localized to a thin layer of width proportional to ε with the help of a phase field function. The resulting problem can be solved using finite elements, where the geometry is now resolved by evaluating the phase field function. This approach was suggested and analyzed in [4, Section 3] in the elliptic case, and in [27] for a linear diffusion equation for a phase field function with nonlocal support. In [16], [17] a phase field function with compact support was used in the approximation of an advection diffusion equation on a moving surface. A corresponding error analysis was carried out in [10] under the simplifying assumption that all occurring integrals can be evaluated exactly. However, as these integrals involve the phase field function, numerical integration needs to be used in practice. The main difficulty in analyzing the effect of numerical integration lies in the fact that corresponding estimates require derivatives of the phase field function, which scale with ε^{-1} . The aim of this paper is to present such an analysis in the elliptic case. We suggest a new, fully practical phase field method to solve (1.1) on a computational domain which consists of a union of elements. For this scheme we derive error bounds in natural norms which clearly reflect the approximation of the solution, the approximation of the geometry as well as the effect of numerical integration, so that the bounds can serve as a guideline on how

to choose the diffuse interface width ε in relation to the grid size h . Furthermore, we present test calculations for hypersurfaces in two and three dimensions which confirm the form of these error bounds.

2 Preliminaries

2.1 Notation and problem formulation

Let $\Gamma \subset \mathbb{R}^{n+1}$ ($n = 1, 2$) be a smooth, connected, compact and orientable hypersurface without boundary. In view of the Jordan-Brouwer separation theorem, Γ divides \mathbb{R}^{n+1} into an interior and an exterior domain and we denote by d the signed distance function to Γ oriented in such a way that $d < 0$ in the interior, $d > 0$ in the exterior of Γ . It is well-known (see [19], Section 14.6) that there exists an open neighbourhood Ω of Γ such that d is smooth in Ω with $|\nabla d(x)| = 1, x \in \Omega$ as well as $\nabla d(x) = \nu(x), x \in \Gamma$, where $\nu(x)$ is the unit outer normal to Γ . Furthermore, the function $\widehat{p}(x) := x - d(x) \nabla d(x)$ assigns to every $x \in \Omega$ the closest point on Γ , so that

$$\widehat{p}(x) \in \Gamma, \quad x - \widehat{p}(x) \perp T_{\widehat{p}(x)}\Gamma \quad \forall x \in \Omega, \quad (2.1)$$

where $T_p\Gamma$ denotes the tangent space at $p \in \Gamma$. Note that $\nabla d(x) = \nabla d(\widehat{p}(x)), x \in \Omega$. For a differentiable function $\eta : \Gamma \rightarrow \mathbb{R}$ let $\nabla_\Gamma \eta(x) = (\underline{D}_1 \eta(x), \dots, \underline{D}_{n+1} \eta(x)) \in T_x \Gamma$ be its tangential gradient. We have that

$$\nabla_\Gamma \eta(x) = \nabla \bar{\eta}(x) - (\nabla \bar{\eta}(x) \cdot \nu(x)) \nu(x) \quad \forall x \in \Gamma, \quad (2.2)$$

where $\bar{\eta}$ is an extension of η to an open neighborhood of Γ . We adopt the standard notation for Sobolev spaces, denoting the norm of $W^{\ell,p}(G)$ ($\ell \in \mathbb{N}, p \in [1, \infty]$ and G a bounded subset in $\mathbb{R}^{n+1}, n = 1, 2$) by $\|\cdot\|_{\ell,p,G}$ and the semi-norm by $|\cdot|_{\ell,p,G}$. If $p = 2$ we write $H^\ell(G) = W^{\ell,2}(G)$ and denote the corresponding norm and semi-norm by $\|\cdot\|_{\ell,G}$ and $|\cdot|_{\ell,G}$ respectively.

Let us consider the following elliptic PDE in divergence form

$$-\sum_{i,j=1}^{n+1} \underline{D}_i (a_{ij} \underline{D}_j u) + a_0 u = f \quad \text{on } \Gamma. \quad (2.3)$$

We assume that $a_{ij} \in C^2(\Gamma)$ and that $A(x) = (a_{ij}(x))_{i,j=1}^{n+1}$ defines a symmetric, uniformly positive definite linear map from $T_x \Gamma$ into itself, so that there exists $\alpha > 0$ with

$$\sum_{i,j=1}^{n+1} a_{ij}(x) \xi_i \nu_j(x) = 0 \quad \forall \xi \in T_x \Gamma, x \in \Gamma; \quad (2.4a)$$

$$\sum_{i,j=1}^{n+1} a_{ij}(x) \xi_i \xi_j \geq \alpha |\xi|^2 \quad \forall \xi \in T_x \Gamma, x \in \Gamma. \quad (2.4b)$$

Since $A(x) \nu(x)$ is not relevant for (2.3), we may assume that $A(x) \nu(x) = \nu(x)$, so that

$$\sum_{i,j=1}^{n+1} a_{ij}(x) \xi_i \xi_j \geq \min\{\alpha, 1\} |\xi|^2 \quad \forall \xi \in \mathbb{R}^{n+1}, x \in \Gamma. \quad (2.5)$$

Furthermore, we suppose that a_0 and f belong to $W^{1,\infty}(\Gamma)$ and that there exists $\alpha_0 > 0$ such that

$$a_0(x) \geq \alpha_0 \quad \forall x \in \Gamma. \quad (2.6)$$

It follows from the Lax–Milgram lemma that for every $f \in L^2(\Gamma)$ the PDE (2.3) has a unique weak solution $u \in H^1(\Gamma)$ in the sense that

$$\sum_{i,j=1}^{n+1} \int_{\Gamma} a_{ij} \underline{D}_j u \underline{D}_i v \, dS_p + \int_{\Gamma} a_0 u v \, dS_p = \int_{\Gamma} f v \, dS_p \quad \forall v \in H^1(\Gamma), \quad (2.7)$$

where dS_p is the surface element of Γ . Furthermore, standard regularity theory implies that $u \in H^2(\Gamma)$ and

$$\|u\|_{2,\Gamma} \leq C \|f\|_{0,\Gamma}. \quad (2.8)$$

In what follows we suppose that Γ is represented in implicit form, i.e. there exists a smooth function $\phi : \bar{\Omega} \rightarrow \mathbb{R}$ such that

$$\Gamma = \{x \in \Omega : \phi(x) = 0\} \quad \text{and} \quad \nabla \phi(x) \neq 0 \quad \forall x \in \Gamma. \quad (2.9)$$

By choosing Ω smaller if necessary we may assume the existence of $c_1 \geq c_0 > 0$ such that

$$c_0 \leq |\nabla \phi(x)| \leq c_1 \quad \forall x \in \bar{\Omega}. \quad (2.10)$$

2.2 Extension

As already mentioned in the introduction our numerical approach is based on extending surface quantities and the surface PDE to a neighborhood of Γ . In what follows we abbreviate

$$U_r := \{x \in \Omega : |\phi(x)| < r\}.$$

A common way to extend a given function $g : \Gamma \rightarrow \mathbb{R}$ consists in setting $\widehat{g}(x) := g(\widehat{p}(x))$, often called the closest-point extension, and we shall use \widehat{p} in order to extend the data a_{ij}, a_0 and f to a neighbourhood of Γ . However, in order to derive our scheme and in order to carry out the error analysis we require a further extension which is better adapted to the level set function ϕ and the diffusion matrix A , see in particular the relation (2.15) below. In what follows we generalize ideas from [9, Section 2.1]. Consider for $p \in \Gamma$ the parameter-dependent system of ODEs

$$\gamma_p'(s) = \frac{A(p) \nabla \phi(\gamma_p(s))}{A(p) \nabla \phi(\gamma_p(s)) \cdot \nabla \phi(\gamma_p(s))}, \quad \gamma_p(0) = p. \quad (2.11)$$

It is not difficult to see that there is $\delta > 0$ such that the solution γ_p of (2.11) exists uniquely on $(-\delta, \delta)$ for every $p \in \Gamma$, so that we may define the mapping $F : \Gamma \times (-\delta, \delta) \rightarrow \mathbb{R}^{n+1}$ by $F(p, s) := \gamma_p(s)$. Recalling that $a_{ij} \in C^2(\Gamma)$ we infer with the help of well-known results on the differentiability of solutions of ODEs with respect to parameters and initial conditions that $F \in C^2(\Gamma \times (-\delta, \delta); \mathbb{R}^{n+1})$. Furthermore, (2.11) implies that

$$\frac{d}{ds} \phi(\gamma_p(s)) = \nabla \phi(\gamma_p(s)) \cdot \gamma_p'(s) = 1,$$

which yields $\phi(\gamma_p(s)) = s$ for $|s| < \delta$, $p \in \Gamma$, since $\phi(\gamma_p(0)) = \phi(p) = 0$. In particular, F is a bijection from $\Gamma \times (-\delta, \delta)$ onto U_δ with inverse

$$F^{-1}(x) = (p(x), \phi(x)) \quad \forall x \in U_\delta, \quad (2.12)$$

where $p \in C^2(U_\delta; \mathbb{R}^{n+1})$ satisfies

$$p(x) \in \Gamma \text{ for } x \in U_\delta \quad \text{and} \quad p(x) = x \text{ for } x \in \Gamma. \quad (2.13)$$

It is not difficult to verify that $p(x) = \widehat{p}(x)$ in the case $A = I$ and $\phi = d$.

Using p we may define an alternative extension for a given $u : \Gamma \rightarrow \mathbb{R}$ to U_δ by setting

$$u^e(x) := u(p(x)) \quad \forall x \in U_\delta. \quad (2.14)$$

It is easily seen that $p(\gamma_p(s)) = p$, $p \in \Gamma$, so that $s \mapsto u^e(\gamma_p(s))$ is constant on $(-\delta, \delta)$. Differentiation with respect to s , together with (2.11), then implies that

$$\nabla u^e(x) \cdot A(p(x)) \nabla \phi(x) = 0 \quad \forall x \in U_\delta. \quad (2.15)$$

Suppose in addition that u is a solution of the surface PDE (2.3). It is shown in Lemma A.4 of the Appendix that u^e then satisfies the uniformly elliptic PDE

$$-\frac{1}{|\nabla \phi|} \nabla \cdot (A^e \nabla u^e |\nabla \phi|) + a_0^e u^e = f^e + \phi R \quad \text{in } U_\delta, \quad (2.16)$$

with $A^e(x) := A(p(x))$, $a_0^e(x) := a_0(p(x))$, $f^e(x) := f(p(x))$ and

$$R(x) = \sum_{1 \leq |\kappa| \leq 2} (b_\kappa(x) + \phi(x) c_\kappa(x)) D_\Gamma^\kappa u(p(x)), \quad (2.17)$$

where $b_\kappa \in C^1(U_\delta)$, $c_\kappa \in C^0(U_\delta)$.

2.3 Phase field approach and finite element approximation

Let us next derive a suitable localized weak formulation of (2.16), which we shall use later in order to formulate our numerical scheme. Let $\sigma \in C^0(\mathbb{R})$ be such that $\sigma(r) > 0$, $|r| < \bar{r}$ and $\sigma(r) = 0$, $|r| \geq \bar{r}$. A concrete choice of σ will be made later. For $\varepsilon \in (0, \frac{\delta}{\bar{r}})$ we define the phase field function

$$\varrho(x) := \sigma\left(\frac{\phi(x)}{\varepsilon}\right) \quad \forall x \in \Omega. \quad (2.18)$$

The restriction on ε ensures that $\text{supp}(\varrho) = \overline{U_{\varepsilon \bar{r}}} \subset U_\delta$. For a function $v \in L^1(\Omega)$ we obtain with the help of the coarea formula

$$\int_\Omega v(x) \varrho(x) |\nabla \phi(x)| dx = \int_{-\varepsilon \bar{r}}^{\varepsilon \bar{r}} \sigma\left(\frac{t}{\varepsilon}\right) \int_{\{\phi=t\}} v(x) dS dt \approx \widehat{c} \varepsilon \int_{\{\phi=0\}} v(x) dS_p \quad (2.19)$$

for small $\varepsilon > 0$, where $\widehat{c} = \int_{-\bar{r}}^{\bar{r}} \sigma(s) ds$. It is therefore reasonable to approximate the surface integral $\int_\Gamma v(x) dS_p$ by the volume integral $(\widehat{c} \varepsilon)^{-1} \int_\Omega v(x) \varrho(x) |\nabla \phi(x)| dx$. The latter expression explains the scaling factor ε^{-1} and the weight $\varrho |\nabla \phi|$, which will frequently occur.

Let us now multiply (2.16) by $v \varrho |\nabla \phi|$ with $v \in H^1(U_r)$ for some $0 < r < \delta$ and integrate over U_r . For the leading term we obtain with the help of integration by parts

$$-\int_{U_r} \nabla \cdot (A^e \nabla u^e |\nabla \phi|) v \varrho \, dx = \int_{U_r} A^e \nabla u^e \cdot \nabla v \varrho |\nabla \phi| \, dx,$$

where we have used (2.15) to see that $A^e \nabla u^e \cdot \nabla \varrho = 0$. For the same reason the boundary term vanishes as the unit outer normal to ∂U_r is a multiple of $\nabla \phi$. Thus, we obtain that

$$\int_{U_r} [A^e \nabla u^e \cdot \nabla v + a_0^e u^e v] \varrho |\nabla \phi| \, dx = \int_{U_r} [f^e + \phi R] v \varrho |\nabla \phi| \, dx \quad \forall v \in H^1(U_r). \quad (2.20)$$

We now use this relation in order to introduce our numerical scheme. To do so, let us assume for simplicity that Ω is polyhedral and denote by \mathcal{T}_h a regular partitioning of Ω into simplices T , i.e.

$$\bar{\Omega} = \bigcup_{T \in \mathcal{T}_h} T. \quad (2.21)$$

We set $h_T := \text{diam}(T)$, $h := \max_{T \in \mathcal{T}_h} h_T$ and let

$$V_h := \{\phi_h \in C^0(\bar{\Omega}) : \phi_h \text{ is affine on } T \text{ for all } T \in \mathcal{T}_h\} \subset H^1(\Omega). \quad (2.22)$$

We denote by $I_h : C^0(\bar{\Omega}) \rightarrow V_h$ the Lagrange interpolation operator. Note for $q > \frac{n+1}{m}$, $m = 1$ or 2 and $\ell = 0$ or 1 that

$$|(I - I_h)v|_{\ell, q, T} \leq C h_T^{m-\ell} |v|_{m, q, T} \quad \forall v \in W^{m, q}(T), \quad \forall T \in \mathcal{T}_h. \quad (2.23)$$

In particular we infer from (2.10) that there exists an $h_0 > 0$ such that for all $h \in (0, h_0]$

$$\frac{c_0}{2} \leq |\nabla I_h \phi(x)| \leq 2c_1 \quad \forall x \in \bar{\Omega}. \quad (2.24)$$

Next, let \hat{T} be the unit simplex in \mathbb{R}^{n+1} and

$$\hat{Q}(\hat{g}) = |\hat{T}| \sum_{i=1}^L \omega_i \hat{g}(\hat{b}_i), \quad \omega_i > 0, \hat{b}_i \in \hat{T}, i = 1, \dots, L$$

a quadrature rule which is exact for all polynomials of degree $\leq q$. This gives rise to a quadrature rule on T via

$$Q_T(g) = |T| \sum_{i=1}^L \omega_i g(b_{i,T}),$$

where $b_{i,T} = \Phi_T(\hat{b}_i) \in T$ and Φ_T is the usual affine transformation from \hat{T} onto T . Using a standard application of the Bramble–Hilbert lemma we obtain for the quadrature error $E_T(g) := Q_T(g) - \int_T g(x) \, dx$ that

$$|E_T(g)| \leq C |T| h_T^{q+1} |g|_{q+1, \infty, T}, \quad g \in W^{q+1, \infty}(T). \quad (2.25)$$

The degree of exactness of the quadrature formula now enters our choice of profile function σ , which we define as

$$\sigma(r) := \begin{cases} \cos^{2(q+1)}(r) & |r| \leq \frac{\pi}{2}, \\ 0 & |r| > \frac{\pi}{2}. \end{cases} \quad (2.26)$$

A straightforward calculation shows that the corresponding phase field function $\varrho(x) = \sigma\left(\frac{\phi(x)}{\varepsilon}\right)$ satisfies for $0 < |\alpha| \leq q + 1$ and $x \in \overline{U_{\varepsilon\frac{\pi}{2}}}$

$$|D^\alpha \varrho(x)| \leq C \sum_{k=1}^{|\alpha|} \varepsilon^{-k} \left| \sigma^{(k)}\left(\frac{\phi(x)}{\varepsilon}\right) \right| \leq C \sum_{k=1}^{|\alpha|} \varepsilon^{-k} \cos^{2(q+1)-k}\left(\frac{\phi(x)}{\varepsilon}\right) \leq C \varepsilon^{-|\alpha|} \varrho(x)^{\frac{2(q+1)-|\alpha|}{2(q+1)}}. \quad (2.27)$$

In order to set up our numerical scheme we define for $h < \varepsilon$

$$\tilde{\mathcal{T}}_h := \left\{ T \in \mathcal{T}_h : |\phi(b_{i,T})| \leq \varepsilon \arccos\left(\frac{h}{\varepsilon}\right) \text{ for all } i = 1, \dots, L \right\}, \quad (2.28)$$

giving rise to the computational domain

$$D_h := \bigcup_{T \in \tilde{\mathcal{T}}_h} T.$$

LEMMA. 2.1. Denote by $r_0 \in (0, 1)$ the unique zero of the function $r \mapsto \arccos(r) - c_1 r$ and suppose that $\varepsilon > 0$ satisfies $\frac{h}{\varepsilon} < r_0$ as well as $c_2 \varepsilon < \delta$, where $c_2 = \frac{\pi}{2} + c_1$ (c_1 as in (2.10)). Let $\hat{\varepsilon} := \varepsilon \arccos\left(\frac{h}{\varepsilon}\right) - c_1 h$. Then $\hat{\varepsilon} > 0$ and

$$\Gamma \subset U_{\hat{\varepsilon}} \subset D_h \subset U_{c_2 \varepsilon} \subset U_\delta. \quad (2.29)$$

Furthermore,

$$\varrho(x) \leq C \left(\frac{h}{\varepsilon}\right)^{2(q+1)}, \quad x \in D_h \setminus U_{\hat{\varepsilon}}. \quad (2.30)$$

Proof. Since $\frac{h}{\varepsilon} < r_0$ and $r \mapsto \arccos(r) - c_1 r$ is strictly decreasing we have

$$\hat{\varepsilon} = \varepsilon \left(\arccos\left(\frac{h}{\varepsilon}\right) - c_1 \frac{h}{\varepsilon} \right) > \varepsilon (\arccos(r_0) - c_1 r_0) = 0.$$

In particular, $\Gamma = \{x \in \Omega : \phi(x) = 0\} \subset U_{\hat{\varepsilon}}$. Next, if $x \in U_{\hat{\varepsilon}} \cap T$, then

$$|\phi(b_{i,T})| \leq |\phi(x)| + |\phi(b_{i,T}) - \phi(x)| < \hat{\varepsilon} + c_1 h = \varepsilon \arccos\left(\frac{h}{\varepsilon}\right), \quad i = 1, \dots, L,$$

which implies that $x \in D_h$. Similarly, we see that $D_h \subset U_{\hat{\varepsilon}}$, where $\tilde{\varepsilon} = \varepsilon \arccos\left(\frac{h}{\varepsilon}\right) + c_1 h \leq c_2 \varepsilon$. It remains to show (2.30) for $x \in D_h \setminus U_{\hat{\varepsilon}}$. We may assume in addition that $x \in \overline{U_{\varepsilon\frac{\pi}{2}}}$ as otherwise $\varrho(x) = 0$. Then we have

$$\cos\left(\frac{\phi(x)}{\varepsilon}\right) \leq \cos\left(\frac{\hat{\varepsilon}}{\varepsilon}\right) = \cos\left(\arccos\left(\frac{h}{\varepsilon}\right) - c_1 \frac{h}{\varepsilon}\right) \leq C \frac{h}{\varepsilon},$$

which yields the desired estimate. \square

Next, let us define the finite element space

$$\tilde{V}_h := \left\{ \phi_h \in C^0(D_h) : \phi_h \text{ is affine on } T \text{ for all } T \in \tilde{\mathcal{T}}_h \right\}. \quad (2.31)$$

For a fixed quadrature rule \hat{Q} and $\varepsilon > 0$ satisfying $\frac{h}{\varepsilon} < r_0$ as well as $c_2 \varepsilon < \delta$ we define the forms a_h and l_h by

$$a_h(v_1, v_2) := \varepsilon^{-1} \sum_{T \in \tilde{\mathcal{T}}_h} Q_T \left[\varrho I_h \hat{A} \nabla v_{1|T} \cdot \nabla v_{2|T} + \varrho I_h \hat{a}_0 v_1 v_2 \right] |\nabla I_h \phi|_T, \quad (2.32a)$$

$$l_h(v) := \varepsilon^{-1} \sum_{T \in \tilde{\mathcal{T}}_h} Q_T \left[\varrho I_h \hat{f} v \right] |\nabla I_h \phi|_T|. \quad (2.32b)$$

In the above, $(I_h \hat{A})_{ij} = I_h \hat{a}_{ij}$, $i, j = 1, \dots, n+1$, and we have abbreviated

$$\hat{A}(x) := A(\hat{p}(x)), \quad \hat{a}_0(x) := a_0(\hat{p}(x)), \quad \hat{f}(x) := f(\hat{p}(x)).$$

We remark that these are used in the scheme rather than A^e , a_0^e and f^e , since in practice the evaluation of \hat{p} is easier compared to p . This is taken into account in the error analysis by controlling the difference $p - \hat{p}$, see Lemma A.3 in the Appendix.

Motivated by (2.20), our fully practical scheme reads: Find $u_h \in \tilde{V}_h$ such that

$$a_h(u_h, v_h) = l_h(v_h) \quad \forall v_h \in \tilde{V}_h, \quad (2.33)$$

REMARK. 2.1. *In contrast to other methods, which require the determination of and integration over an approximate surface Γ_h or a suitable narrow band, the implementation of (2.33) is rather straightforward. The underlying geometry is incorporated through the level set function ϕ and the projection \hat{p} . Note that \hat{p} is only required at the grid points of $\tilde{\mathcal{T}}_h$.*

Let us introduce

$$\|v_h\|_h := \left(\varepsilon^{-1} \sum_{T \in \tilde{\mathcal{T}}_h} Q_T \left[\varrho (|v_h|^2 + |\nabla v_h|_T^2) \right] \right)^{\frac{1}{2}}, \quad v_h \in \tilde{V}_h. \quad (2.34)$$

In view of (2.24), (2.5) and (2.6) there exists $c_3 > 0$, which is independent of h , such that

$$c_3 \|v_h\|_h^2 \leq a_h(v_h, v_h) \quad \text{for all } v_h \in \tilde{V}_h. \quad (2.35)$$

In particular we have:

LEMMA. 2.2. *The discrete problem (2.33) has a unique solution $u_h \in \tilde{V}_h$ for all $0 < h < \varepsilon$, $c_2 \varepsilon < \delta$.*

Proof. It is sufficient to verify that the homogeneous problem only has the trivial solution. Hence suppose that $a_h(u_h, v_h) = 0$ for all $v_h \in \tilde{V}_h$. Inserting $v_h = u_h$ and using (2.35) we infer

$$\sum_{T \in \tilde{\mathcal{T}}_h} \sum_{i=1}^L \omega_i \varrho(b_{i,T}) (|u_h(b_{i,T})|^2 + |\nabla u_h|_T|^2) |T| = 0.$$

The definition of $\tilde{\mathcal{T}}_h$ yields

$$\varrho(b_{i,T}) = \cos^{2(q+1)} \left(\frac{\phi(b_{i,T})}{\varepsilon} \right) \geq \left(\frac{h}{\varepsilon} \right)^{2(q+1)} \quad \text{for all } i = 1, \dots, L, T \in \tilde{\mathcal{T}}_h, \quad (2.36)$$

so that $\nabla u_h|_T \equiv 0$, $u_h(b_{i,T}) = 0$ for all $i = 1, \dots, L$ and all $T \in \tilde{\mathcal{T}}_h$. Hence $u_h \equiv 0$ in D_h . \square

Let us formulate the main result of this paper.

THEOREM. 2.1. *Let $u \in H^2(\Gamma)$ be the unique solution of (2.3) extended to u^e via (2.14) and $u_h \in \tilde{V}_h$ the unique solution of (2.33). Then*

$$\|I_h u^e - u_h\|_h \leq C \left(h + \varepsilon^2 + \left(\frac{h}{\varepsilon}\right)^{q+1} \right) (\|u\|_{2,\Gamma} + \|f\|_{1,\infty,\Gamma}). \quad (2.37)$$

If in addition there exists a constant $c_4 > 0$ which is independent of h such that $c_4 h \leq h_T$ for all $T \in \mathcal{T}_h$ with $|T \cap \Gamma| > 0$, then

$$\|u - u_h\|_{1,\Gamma} \leq C \sqrt{\frac{\varepsilon}{h}} \left(h + \varepsilon^2 + \left(\frac{h}{\varepsilon}\right)^{q+1} \right) (\|u\|_{2,\Gamma} + \|f\|_{1,\infty,\Gamma}). \quad (2.38)$$

The proof of these results will be given in the next section.

REMARK. 2.2. *The three terms on the right hand side of (2.37) are related to the different approximations that are used in the discretization. The first term is due to the use of piecewise linear finite elements in order to discretize the solution and the level set function, while the second term arises from working with the extended PDE in a narrow band of width ε . Finally, $\left(\frac{h}{\varepsilon}\right)^{q+1}$ reflects how well integrals involving the phase field function are approximated via the quadrature rule. Note that the quotient $\frac{\varepsilon}{h} > 1$ roughly measures how many grid points are used across the narrow band.*

REMARK. 2.3. *For a fixed degree of accuracy $q \geq 1$, let us choose $\varepsilon = h^\theta$, where $\theta = \frac{q+1}{q+3} < 1$. Since $2\theta = (1 - \theta)(q + 1) \geq 1$, (2.37) and (2.38) yield*

$$\|I_h u^e - u_h\|_h \leq C (h + h^{2\theta}) \leq Ch, \quad \|u - u_h\|_{1,\Gamma} \leq Ch^{\frac{\theta-1}{2}} h = Ch^{\frac{q+2}{q+3}}.$$

Thus, we have convergence for both norms as $h \rightarrow 0$ and $\varepsilon = h^\theta$.

3 Error Analysis

Before we start with the actual error analysis, we first prove a useful auxiliary result.

LEMMA. 3.1.

$$\varepsilon^{-1} \sum_{T \in \tilde{\mathcal{T}}_h} |\varrho|_{0,\infty,T} \|v_h\|_{1,T}^2 \leq C \|v_h\|_h^2, \quad \forall v_h \in \tilde{V}_h. \quad (3.1)$$

Proof. Let us fix $T \in \tilde{\mathcal{T}}_h$. Using (2.27) and Young's inequality we have for every $x \in T$

$$\begin{aligned} \varrho(x) &\leq \varrho(b_{i,T}) + |\nabla \varrho|_{0,\infty,T} |x - b_{i,T}| \leq \varrho(b_{i,T}) + C \frac{h_T}{\varepsilon} |\varrho|_{0,\infty,T}^{\frac{2(q+1)-1}{2(q+1)}} \\ &\leq \varrho(b_{i,T}) + \frac{1}{2} |\varrho|_{0,\infty,T} + C \left(\frac{h}{\varepsilon}\right)^{2(q+1)}. \end{aligned}$$

Taking the maximum with respect to x and recalling (2.36) we infer that

$$|\varrho|_{0,\infty,T} \leq C \varrho(b_{i,T}), \quad i = 1, \dots, L. \quad (3.2)$$

To proceed, we choose $x_T \in T$ such that $|v_h(x_T)| = |v_h|_{0,\infty,T}$ and have, as ∇v_h is constant on T , that $|v_h(x_T)| \leq |v_h(b_{i,T})| + h_T |\nabla v_h|_T$ for $i = 1, \dots, L$. Hence, we deduce

$$\|v_h\|_{1,T}^2 \leq (|v_h(x_T)|^2 + |\nabla v_h|_T^2) |T| \leq C(|v_h(b_{i,T})|^2 + |\nabla v_h|_T^2) |T|, \quad i = 1, \dots, L.$$

Combining this bound with (3.2) and observing that $\sum_{i=1}^L \omega_i = 1$ we obtain

$$|\varrho|_{0,\infty,T} \|v_h\|_{1,T}^2 \leq C \sum_{i=1}^L \omega_i \varrho(b_{i,T}) (|v_h(b_{i,T})|^2 + |\nabla v_h|_T^2) |T| = C Q_T [\varrho(|v_h|^2 + |\nabla v_h|_T^2)],$$

which concludes the proof of the lemma after summation over $T \in \tilde{\mathcal{T}}_h$. \square

Let us now start the proof of the error bound. Define $e_h := (I_h u^e)|_{D_h} - u_h \in \tilde{V}_h$. We infer from (2.35) and (2.33)

$$c_3 \|e_h\|_h^2 \leq a_h(e_h, e_h) = a_h(I_h u^e, e_h) - l_h(e_h) =: S_1 + S_2. \quad (3.3)$$

Recalling the definition of a_h we may write

$$\begin{aligned} S_1 &= \varepsilon^{-1} \sum_{T \in \tilde{\mathcal{T}}_h} \left\{ Q_T \left[\varrho I_h \hat{A} \nabla I_h u^e|_T \cdot \nabla e_h|_T + \varrho I_h \hat{a}_0 I_h u^e e_h \right] \right. \\ &\quad \left. - \int_T \left[\varrho I_h \hat{A} \nabla I_h u^e|_T \cdot \nabla e_h|_T + \varrho I_h \hat{a}_0 I_h u^e e_h \right] dx \right\} |\nabla I_h \phi|_T \\ &\quad + \varepsilon^{-1} \int_{D_h} (\varrho I_h \hat{A} \nabla (I_h u^e - u^e) \cdot \nabla e_h + \varrho I_h \hat{a}_0 (I_h u^e - u^e) e_h) |\nabla I_h \phi| dx \\ &\quad + \varepsilon^{-1} \int_{D_h} (\varrho (I_h \hat{A} - \hat{A}) \nabla u^e \cdot \nabla e_h + \varrho (I_h \hat{a}_0 - \hat{a}_0) u^e e_h) |\nabla I_h \phi| dx \\ &\quad + \varepsilon^{-1} \int_{D_h} \varrho \left[\hat{A} \nabla u^e \cdot \nabla e_h + \hat{a}_0 u^e e_h \right] [|\nabla I_h \phi| - |\nabla \phi|] dx \\ &\quad + \varepsilon^{-1} \int_{D_h} \varrho \left[(\hat{A} - A^e) \nabla u^e \cdot \nabla e_h + (\hat{a}_0 - a_0^e) u^e e_h \right] |\nabla \phi| dx \\ &\quad + \varepsilon^{-1} \int_{D_h} [A^e \nabla u^e \cdot \nabla e_h + a_0^e u^e e_h] \varrho |\nabla \phi| dx =: \sum_{i=1}^6 S_{1,i}. \end{aligned}$$

Using (2.25) and (2.24) we obtain

$$\begin{aligned} |S_{1,1}| &\leq \varepsilon^{-1} \sum_{T \in \tilde{\mathcal{T}}_h} \left\{ |E_T(\varrho I_h \hat{A})| |\nabla I_h u^e|_T |\nabla e_h|_T + |E_T(\varrho I_h \hat{a}_0 I_h u^e e_h)| \right\} \\ &\leq C \varepsilon^{-1} \sum_{T \in \tilde{\mathcal{T}}_h} |T| h_T^{q+1} \left\{ |\varrho I_h \hat{A}|_{q+1,\infty,T} |\nabla I_h u^e|_T |\nabla e_h|_T + |\varrho I_h \hat{a}_0 I_h u^e e_h|_{q+1,\infty,T} \right\} \\ &\leq C \varepsilon^{-1} \sum_{T \in \tilde{\mathcal{T}}_h} |T| h_T^{q+1} \|\varrho\|_{q+1,\infty,T} (\|I_h \hat{A}\|_{1,\infty,T} + \|I_h \hat{a}_0\|_{1,\infty,T}) \|I_h u^e\|_{1,\infty,T} \|e_h\|_{1,\infty,T} \\ &\leq C \varepsilon^{-1} \sum_{T \in \tilde{\mathcal{T}}_h} h_T^{q+1} \|\varrho\|_{q+1,\infty,T} \|I_h u^e\|_{1,T} \|e_h\|_{1,T} \end{aligned}$$

where the last bound follows from an inverse estimate and the fact that a_{ij}, a_0 are Lipschitz on Γ . Applying (2.27) and using (3.1), (2.23), (2.29) and (A.3) we deduce

$$\begin{aligned}
|S_{1,1}| &\leq C\varepsilon^{-1} \sum_{T \in \tilde{\mathcal{T}}_h} h_T^{q+1} \varepsilon^{-(q+1)} |\varrho|_{0,\infty,T}^{\frac{1}{2}} \|I_h u^e\|_{1,T} \|e_h\|_{1,T} \\
&\leq C \left(\frac{h}{\varepsilon}\right)^{q+1} \left(\varepsilon^{-1} \sum_{T \in \tilde{\mathcal{T}}_h} \|I_h u^e\|_{1,T}^2 \right)^{\frac{1}{2}} \left(\varepsilon^{-1} \sum_{T \in \tilde{\mathcal{T}}_h} |\varrho|_{0,\infty,T} \|e_h\|_{1,T}^2 \right)^{\frac{1}{2}} \\
&\leq C \left(\frac{h}{\varepsilon}\right)^{q+1} \left(\varepsilon^{-1} \sum_{T \in \tilde{\mathcal{T}}_h} \|u^e\|_{2,T}^2 \right)^{\frac{1}{2}} \|e_h\|_h \\
&\leq C \left(\frac{h}{\varepsilon}\right)^{q+1} \varepsilon^{-\frac{1}{2}} \|u^e\|_{2,U_{c_2\varepsilon}} \|e_h\|_h \leq C \left(\frac{h}{\varepsilon}\right)^{q+1} \|u\|_{2,\Gamma} \|e_h\|_h.
\end{aligned} \tag{3.4}$$

Using similar arguments we deduce that

$$\begin{aligned}
|S_{1,2}| &\leq C\varepsilon^{-1} \sum_{T \in \tilde{\mathcal{T}}_h} |\varrho|_{0,\infty,T} \|I_h u^e - u^e\|_{1,T} \|e_h\|_{1,T} \\
&\leq Ch \left(\varepsilon^{-1} \sum_{T \in \tilde{\mathcal{T}}_h} |u^e|_{2,T}^2 \right)^{\frac{1}{2}} \left(\varepsilon^{-1} \sum_{T \in \tilde{\mathcal{T}}_h} |\varrho|_{0,\infty,T} \|e_h\|_{1,T}^2 \right)^{\frac{1}{2}} \\
&\leq Ch \|u\|_{2,\Gamma} \|e_h\|_h
\end{aligned} \tag{3.5}$$

as well as

$$\begin{aligned}
|S_{1,3}| + |S_{1,4}| &\leq C\varepsilon^{-1} \sum_{T \in \tilde{\mathcal{T}}_h} |\varrho|_{0,\infty,T} h_T (\widehat{A}|_{1,\infty,T} + |\widehat{a}_0|_{1,\infty,T} + |\phi|_{2,\infty,T}) \|u^e\|_{1,T} \|e_h\|_{1,T} \\
&\leq Ch \left(\varepsilon^{-1} \sum_{T \in \tilde{\mathcal{T}}_h} \|u^e\|_{1,T}^2 \right)^{\frac{1}{2}} \left(\varepsilon^{-1} \sum_{T \in \tilde{\mathcal{T}}_h} |\varrho|_{0,\infty,T} \|e_h\|_{1,T}^2 \right)^{\frac{1}{2}} \\
&\leq Ch \|u\|_{1,\Gamma} \|e_h\|_h.
\end{aligned} \tag{3.6}$$

Since $A \in C^1(\Gamma)$, it follows from (A.12) and (2.29) that for $x \in D_h$

$$|\widehat{A}(x) - A^e(x)| = |A(\widehat{p}(x)) - A(p(x))| \leq C |\widehat{p}(x) - p(x)| \leq C \phi(x)^2 \leq C\varepsilon^2$$

and, similarly, $|\widehat{a}_0(x) - a_0^e(x)| \leq C\varepsilon^2$. This implies together with (3.1) and (A.3)

$$\begin{aligned}
|S_{1,5}| &\leq C\varepsilon \int_{D_h} \varrho [|\nabla u^e| + |u^e|] [|\nabla e_h| + |e_h|] dx \\
&\leq C\varepsilon^2 \left(\varepsilon^{-1} \sum_{T \in \tilde{\mathcal{T}}_h} \|u^e\|_{1,T}^2 \right)^{\frac{1}{2}} \left(\varepsilon^{-1} \sum_{T \in \tilde{\mathcal{T}}_h} |\varrho|_{0,\infty,T} \|e_h\|_{1,T}^2 \right)^{\frac{1}{2}} \\
&\leq C\varepsilon^2 \varepsilon^{-\frac{1}{2}} \|u^e\|_{1,U_{c_2\varepsilon}} \|e_h\|_h \leq C\varepsilon^2 \|u\|_{1,\Gamma} \|e_h\|_h.
\end{aligned} \tag{3.7}$$

Combining (3.4)–(3.7) we infer that

$$S_1 \leq C \left(h + \varepsilon^2 + \left(\frac{h}{\varepsilon}\right)^{q+1} \right) \|u\|_{2,\Gamma} \|e_h\|_h + \varepsilon^{-1} \int_{D_h} [A^e \nabla u^e \cdot \nabla e_h + a_0^e u^e e_h] \varrho |\nabla \phi| dx. \tag{3.8}$$

Next, it follows from (2.32b) that

$$\begin{aligned} S_2 &= \varepsilon^{-1} \sum_{T \in \tilde{\mathcal{T}}_h} \left\{ \int_T \varrho I_h \hat{f} e_h \, dx - Q_T(\varrho I_h \hat{f} e_h) \right\} |\nabla I_h \phi|_T + \varepsilon^{-1} \int_{D_h} \varrho(\hat{f} - I_h \hat{f}) e_h |\nabla I_h \phi| \, dx \\ &\quad + \varepsilon^{-1} \int_{D_h} \varrho \hat{f} e_h [|\nabla \phi| - |\nabla I_h \phi|] \, dx + \varepsilon^{-1} \int_{D_h} \varrho [f^e - \hat{f}] e_h |\nabla \phi| \, dx - \varepsilon^{-1} \int_{D_h} f^e e_h \varrho |\nabla \phi| \, dx. \end{aligned}$$

Arguing in a similar way as for $S_{1,i}$, $i = 1, 3, 4, 5$, we obtain

$$S_2 \leq C \left(h + \varepsilon^2 + \left(\frac{h}{\varepsilon}\right)^{q+1} \right) \|f\|_{1,\infty,\Gamma} \|e_h\|_h - \varepsilon^{-1} \int_{D_h} f^e e_h \varrho |\nabla \phi| \, dx \quad (3.9)$$

and hence

$$S_1 + S_2 \leq C \left(h + \varepsilon^2 + \left(\frac{h}{\varepsilon}\right)^{q+1} \right) [\|f\|_{1,\infty,\Gamma} + \|u\|_{2,\Gamma}] \|e_h\|_h + S_3, \quad (3.10)$$

where

$$\begin{aligned} S_3 &:= \varepsilon^{-1} \int_{D_h} [A^e \nabla u^e \cdot \nabla e_h + a_0^e u^e e_h - f^e e_h] \varrho |\nabla \phi| \, dx \\ &= \varepsilon^{-1} \left(\int_{U_\varepsilon} + \int_{D_h \setminus U_\varepsilon} \right) [A^e \nabla u^e \cdot \nabla e_h + a_0^e u^e e_h - f^e e_h] \varrho |\nabla \phi| \, dx = I + II. \end{aligned} \quad (3.11)$$

If we apply (2.20) with $r = \hat{\varepsilon}$ and use the transformation F introduced in Section 2.2 we obtain upon recalling that $\phi(F(p, s)) = s$

$$\begin{aligned} I &= \varepsilon^{-1} \int_{U_\varepsilon} \phi R e_h \varrho |\nabla \phi| \, dx \\ &= \varepsilon^{-1} \int_{-\hat{\varepsilon}}^{\hat{\varepsilon}} s \sigma \left(\frac{s}{\varepsilon} \right) \int_{\Gamma} R(F(p, s)) e_h(F(p, s)) |\nabla \phi(F(p, s))| \mu(p, s) \, dS_p \, ds. \end{aligned} \quad (3.12)$$

Here, $\mu(p, s)$ is the Jacobian determinant of F , which satisfies

$$\left| \mu(p, s) - \frac{1}{|\nabla \phi(F(p, s))|} \right| \leq C |s| \quad \text{for } p \in \Gamma, |s| < \hat{\varepsilon}. \quad (3.13)$$

Since $\int_{-\hat{\varepsilon}}^{\hat{\varepsilon}} s \sigma \left(\frac{s}{\varepsilon} \right) \, ds = 0$, we deduce from (3.12) that

$$\begin{aligned} I &= \varepsilon^{-1} \int_{-\hat{\varepsilon}}^{\hat{\varepsilon}} s \sigma \left(\frac{s}{\varepsilon} \right) \int_{\Gamma} [R(F(p, s)) |\nabla \phi(F(p, s))| \mu(p, s) - R(p)] e_h(F(p, s)) \, dS_p \, ds \\ &\quad + \varepsilon^{-1} \int_{-\hat{\varepsilon}}^{\hat{\varepsilon}} s \sigma \left(\frac{s}{\varepsilon} \right) \int_{\Gamma} [e_h(F(p, s)) - e_h(p)] R(p) \, dS_p \, ds =: I_1 + I_2. \end{aligned} \quad (3.14)$$

Recalling the form of R , (2.17), as well as $p(F(p, s)) = p$ for $p \in \Gamma$, we have

$$R(F(p, s)) = \sum_{1 \leq |\kappa| \leq 2} (b_\kappa(F(p, s)) + s c_\kappa(F(p, s))) D_\Gamma^\kappa u(p),$$

so that since $F(p, 0) = p$ and $b_\kappa \in C^1$, $c_\kappa \in C^0$

$$|R(F(p, s)) - R(p)| \leq C |s| \sum_{1 \leq |\kappa| \leq 2} |D_\Gamma^\kappa u(p)| \quad \forall p \in \Gamma, |s| < \hat{\varepsilon}.$$

Combining this bound with (3.13) we infer that

$$\begin{aligned}
|I_1| &\leq C \varepsilon^{-1} \int_{-\widehat{\varepsilon}}^{\widehat{\varepsilon}} s^2 \sigma\left(\frac{s}{\varepsilon}\right) \int_{\Gamma} [|\nabla_{\Gamma} u(p)| + |D_{\Gamma}^2 u(p)|] |e_h(F(p, s))| dS_p ds \\
&\leq C \varepsilon^2 \|u\|_{2,\Gamma} \left(\varepsilon^{-1} \int_{-\widehat{\varepsilon}}^{\widehat{\varepsilon}} \sigma\left(\frac{s}{\varepsilon}\right) \int_{\Gamma} |e_h(F(p, s))|^2 dS_p ds \right)^{\frac{1}{2}}.
\end{aligned} \tag{3.15}$$

Similarly, we have that

$$\begin{aligned}
|I_2| &\leq \varepsilon^{-1} \int_{-\widehat{\varepsilon}}^{\widehat{\varepsilon}} |s| \sigma\left(\frac{s}{\varepsilon}\right) \int_{\Gamma} |e_h(F(p, s)) - e_h(p)| |R(p)| dS_p ds \\
&\leq C \int_{-\widehat{\varepsilon}}^{\widehat{\varepsilon}} \sigma\left(\frac{s}{\varepsilon}\right) \int_{\Gamma} |R(p)| \left| \int_0^s |\nabla e_h(F(p, t))| dt \right| dS_p ds \\
&\leq C \varepsilon \int_{-\widehat{\varepsilon}}^{\widehat{\varepsilon}} \sigma\left(\frac{t}{\varepsilon}\right) \int_{\Gamma} |\nabla e_h(F(p, t))| |R(p)| dS_p dt \\
&\leq C \varepsilon^2 \|u\|_{2,\Gamma} \left(\varepsilon^{-1} \int_{-\widehat{\varepsilon}}^{\widehat{\varepsilon}} \sigma\left(\frac{s}{\varepsilon}\right) \int_{\Gamma} |\nabla e_h(F(p, s))|^2 dS_p ds \right)^{\frac{1}{2}},
\end{aligned} \tag{3.16}$$

where we have used again (2.17) as well as the fact that $\sigma\left(\frac{s}{\varepsilon}\right) \leq \sigma\left(\frac{t}{\varepsilon}\right)$ for $|t| \leq |s| \leq \widehat{\varepsilon}$. Combining (3.14)–(3.16) and applying once more the transformation rule together with (2.29) and (3.1) we obtain

$$|I| \leq C \varepsilon^2 \|u\|_{2,\Gamma} \left(\varepsilon^{-1} \int_{D_h} \varrho(|e_h|^2 + |\nabla e_h|^2) dx \right)^{\frac{1}{2}} \leq C \varepsilon^2 \|u\|_{2,\Gamma} \|e_h\|_h. \tag{3.17}$$

Since $\varrho(x) \leq C\left(\frac{h}{\varepsilon}\right)^{q+1} \sqrt{\varrho(x)}$, $x \in D_h \setminus U_{\widehat{\varepsilon}}$ in view of (2.30) we have

$$\begin{aligned}
|II| &\leq C\left(\frac{h}{\varepsilon}\right)^{q+1} \varepsilon^{-1} \int_{D_h \setminus U_{\widehat{\varepsilon}}} (|\nabla u^e| + |u^e| + |f^e|) \sqrt{\varrho} (|\nabla e_h| + |e_h|) dx \\
&\leq C\left(\frac{h}{\varepsilon}\right)^{q+1} \left(\varepsilon^{-1} \int_{U_{C_2\varepsilon}} (|\nabla u^e|^2 + |u^e|^2 + |f^e|^2) dx \right)^{\frac{1}{2}} \left(\varepsilon^{-1} \int_{D_h} \varrho (|\nabla e_h|^2 + |e_h|^2) dx \right)^{\frac{1}{2}} \\
&\leq C\left(\frac{h}{\varepsilon}\right)^{q+1} (\|u\|_{1,\Gamma} + \|f\|_{0,\Gamma}) \|e_h\|_h.
\end{aligned}$$

Inserting the above bounds into (3.11) we derive

$$S_3 \leq C \left(\varepsilon^2 + \left(\frac{h}{\varepsilon}\right)^{q+1} \right) (\|u\|_{2,\Gamma} + \|f\|_{0,\Gamma}) \|e_h\|_h, \tag{3.18}$$

so that (3.3) and (3.10) yield

$$\|e_h\|_h \leq C \left(h + \varepsilon^2 + \left(\frac{h}{\varepsilon}\right)^{q+1} \right) (\|u\|_{2,\Gamma} + \|f\|_{1,\infty,\Gamma}),$$

proving (2.37). In order to show (2.38) we shall make use of the following trace–type inequality for $T \in \mathcal{T}_h$, which is a consequence of [21, Lemma 3] and [22, Lemma 3]:

$$\|v\|_{0,T \cap \Gamma}^2 \leq C(h_T^{-1} \|v\|_{0,T}^2 + h_T \|\nabla v\|_{0,T}^2) \quad \text{for all } v \in H^1(T). \tag{3.19}$$

If we combine this estimate with (2.23), the fact that $|\varrho|_{0,\infty,T} = 1$ if $T \cap \Gamma \neq \emptyset$ and (2.29) we infer that

$$\begin{aligned} \|u - u_h\|_{1,\Gamma}^2 &= \sum_{|T \cap \Gamma| > 0} \|u - u_h\|_{1,T \cap \Gamma}^2 = \sum_{|T \cap \Gamma| > 0} \|u^e - u_h\|_{1,T \cap \Gamma}^2 \\ &\leq C \sum_{|T \cap \Gamma| > 0} (h_T^{-1} \|u^e - u_h\|_{1,T}^2 + h_T \|u^e\|_{2,T}^2) \leq C \sum_{|T \cap \Gamma| > 0} h_T^{-1} |\varrho|_{0,\infty,T} \|I_h u^e - u_h\|_{1,T}^2 + Ch \|u^e\|_{2,U_{c_2\varepsilon}}^2. \end{aligned}$$

Finally, using the assumption that $c_4 h \leq h_T$ for all $T \in \mathcal{T}_h$ with $|T \cap \Gamma| > 0$, (3.1) and (A.3) we deduce

$$\begin{aligned} \|u - u_h\|_{1,\Gamma}^2 &\leq C \frac{\varepsilon}{h} \sum_{|T \cap \Gamma| > 0} \varepsilon^{-1} |\varrho|_{0,\infty,T} \|I_h u^e - u_h\|_{1,T}^2 + Ch \varepsilon \|u\|_{2,\Gamma}^2 \\ &\leq C \frac{\varepsilon}{h} (\|I_h u^e - u_h\|_h^2 + Ch^2 \|u\|_{2,\Gamma}^2) \end{aligned}$$

from which we infer (2.38) with the help of (2.37).

4 Numerical Experiments

We investigate the experimental order of convergence (eoc) for the following errors:

$$\mathcal{E}_1 = \varepsilon^{-1} \sum_{T \in \tilde{\mathcal{T}}_h} Q_T [\varrho |I_h u^e - u_h|^2] \quad \text{and} \quad \mathcal{E}_2 = \varepsilon^{-1} \sum_{T \in \tilde{\mathcal{T}}_h} Q_T [\varrho |\nabla(I_h u^e - u_h)|^2].$$

The corresponding calculations will be done for a circle (Example 1) and a sphere (Example 2) of radius 1, described as the zero level set of the function $\phi(x) := |x|^2 - 1$. In this case one can verify without difficulty that the projection p constructed in Section 2.2 coincides with the closest point projection \hat{p} , so that we have $u^e(x) = u(\frac{x}{|x|})$ for $x \neq 0$. We use the finite element toolbox Alberta 2.0, [30], and implement a similar mesh refinement strategy to that in [1] with a fine mesh constructed in D_h and a coarser mesh in $\Omega \setminus D_h$. The resulting linear systems were solved using CG together with diagonal preconditioning. In all the examples we consider we set $a_{ij} = \delta_{ij}$, $i, j = 1, \dots, n+1$ and $a_0 = 1$ in (2.3). For the values of q given in the examples below, we implement quadrature rules that are exact up to order q .

Example 1

Let $\Omega = (-1.2, 1.2)^2$ and take $\Gamma = \{x \in \mathbb{R}^2 \mid |x| = 1\}$ to be a circle of radius 1, described as the zero level set of the function $\phi(x) := x_1^2 + x_2^2 - 1$. In addition to $\mathcal{E}_1, \mathcal{E}_2$ we shall also investigate the errors appearing in (2.38). To do so, we approximate $\|u - u_h\|_{L^2(\Gamma)}^2$ and $\|\nabla_\Gamma(u - u_h)\|_{L^2(\Gamma)}^2$ by

$$\mathcal{E}_3 = \sum_{l=0}^{\Lambda-1} \frac{2\pi}{\Lambda} |u(x_l) - u_h(x_l)|^2 \quad \text{and} \quad \mathcal{E}_4 = \sum_{l=0}^{\Lambda-1} \frac{2\pi}{\Lambda} |\nabla_\Gamma u(x_l) - \nabla_\Gamma u_h(x_l)|^2$$

respectively, where we have chosen the quadrature points

$$x_l := \left(\cos\left(\frac{2\pi l}{\Lambda}\right), \sin\left(\frac{2\pi l}{\Lambda}\right) \right)^T, \quad l = 0, \dots, \Lambda - 1.$$

In our computations taking $\Lambda = 200$ was sufficient in order to observe the expected eocs. We choose f so that $u(x) := (x_1^2 - x_2^2)/|x|^2$ solves (2.3) and fixed $\varepsilon = 5.333h$. In Tables 1 – 3 we display the values of \mathcal{E}_i , $i = 1, \dots, 4$, together with the eocs, for $q = 1$, $q = 2$ and $q = 7$ respectively. For the smaller values $q = 1$ and $q = 2$ we observe an eoc for \mathcal{E}_2 which is lower than two indicating that in this case the term $(\frac{h}{\varepsilon})^{q+1}$ in (2.37) dominates. This effect disappears for the choice $q = 7$, where we see eocs close to two for \mathcal{E}_2 and \mathcal{E}_4 . Furthermore, we observe eocs close to four for \mathcal{E}_1 and \mathcal{E}_3 suggesting that the error analysis can be improved for the L^2 -errors. In Figure 1 we display the positive quadrant of three meshes, $h = 3.750e-02$ (left), $h = 9.375e-03$ (centre) and $h = 2.344e-03$ (right), the triangulation $\tilde{\mathcal{T}}_h$ can be identified by the region where the mesh is fine.

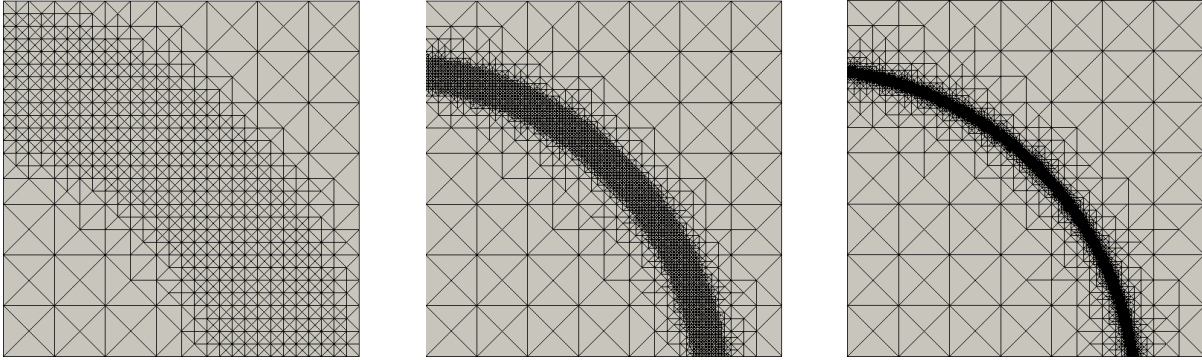


Figure 1: The positive quadrants of three of the meshes from Example 1, $h = 3.750e-02$ (left), $h = 9.375e-03$ (centre) and $h = 2.344e-03$ (right).

| h | ε | \mathcal{E}_1 | eoc_1 | \mathcal{E}_2 | eoc_2 | \mathcal{E}_3 | eoc_3 | \mathcal{E}_4 | eoc_4 |
|-----------|---------------|-----------------|---------|-----------------|---------|-----------------|---------|-----------------|---------|
| 3.750e-02 | 0.2 | 4.853e-05 | - | 1.911e-03 | - | 7.657e-05 | - | 1.568e-02 | - |
| 1.875e-02 | 0.1 | 2.869e-06 | 4.08 | 4.469e-04 | 2.10 | 4.713e-06 | 4.02 | 3.845e-03 | 2.03 |
| 9.375e-03 | 0.05 | 1.712e-07 | 4.07 | 2.584e-04 | 0.79 | 2.755e-07 | 4.10 | 9.847e-04 | 1.97 |
| 4.687e-03 | 0.025 | 9.618e-09 | 4.15 | 1.759e-04 | 0.56 | 1.577e-08 | 4.13 | 2.436e-04 | 2.02 |
| 2.344e-03 | 0.0125 | 1.675e-10 | 5.84 | 1.837e-04 | -0.06 | 1.347e-10 | 6.87 | 6.098e-05 | 2.00 |

Table 1: Example 1, errors and experimental orders of convergence, $q = 1$.

| h | ε | \mathcal{E}_1 | eoc_1 | \mathcal{E}_2 | eoc_2 | \mathcal{E}_3 | eoc_3 | \mathcal{E}_4 | eoc_4 |
|-----------|---------------|-----------------|---------|-----------------|---------|-----------------|---------|-----------------|---------|
| 3.750e-02 | 0.2 | 2.150e-05 | - | 1.152e-03 | - | 3.867e-05 | - | 1.555e-02 | - |
| 1.875e-02 | 0.1 | 1.356e-06 | 3.99 | 2.110e-04 | 2.45 | 2.500e-06 | 3.95 | 3.797e-03 | 2.03 |
| 9.375e-03 | 0.05 | 7.591e-08 | 4.16 | 9.743e-05 | 1.11 | 1.390e-07 | 4.17 | 9.703e-04 | 1.97 |
| 4.687e-03 | 0.025 | 4.259e-09 | 4.16 | 9.435e-05 | 0.05 | 7.079e-09 | 4.30 | 2.400e-04 | 2.02 |
| 2.344e-03 | 0.0125 | 1.806e-10 | 4.56 | 6.677e-05 | 0.50 | 1.721e-10 | 5.36 | 6.007e-05 | 2.00 |

Table 2: Example 1, errors and experimental orders of convergence, $q = 2$.

| h | ε | \mathcal{E}_1 | eoc_1 | \mathcal{E}_2 | eoc_2 | \mathcal{E}_3 | eoc_3 | \mathcal{E}_4 | eoc_4 |
|-----------|---------------|-----------------|---------|-----------------|---------|-----------------|---------|-----------------|---------|
| 3.750e-02 | 0.2 | 3.211e-06 | - | 4.139e-04 | - | 8.768e-06 | - | 1.535e-02 | - |
| 1.875e-02 | 0.1 | 1.999e-07 | 4.01 | 8.996e-05 | 2.20 | 5.499e-07 | 4.00 | 3.722e-03 | 2.04 |
| 9.375e-03 | 0.05 | 1.248e-08 | 4.00 | 2.166e-05 | 2.05 | 3.440e-08 | 4.00 | 9.481e-04 | 1.97 |
| 4.687e-03 | 0.025 | 7.801e-10 | 4.00 | 5.368e-06 | 2.01 | 2.154e-09 | 4.00 | 2.345e-04 | 2.02 |
| 2.344e-03 | 0.0125 | 4.883e-11 | 4.00 | 1.344e-06 | 2.00 | 1.351e-10 | 4.00 | 5.867e-05 | 2.00 |

Table 3: Example 1, errors and experimental orders of convergence, $q = 7$.

Example 2

We set $\Omega = (-2.42, 2.42)^3$ and take $\Gamma = \{x \in \mathbb{R}^3 \mid |x| = 1\}$ to be a sphere of radius 1, described as the zero level set of the function $\phi(x) := x_1^2 + x_2^2 + x_3^2 - 1$. As in Example 1, in addition to $\mathcal{E}_1, \mathcal{E}_2$ we shall also investigate the errors appearing in (2.38) which we approximate by the quadrature rules

$$\mathcal{E}_3 = \sum_{k=0}^{2\Lambda-1} \sum_{l=0}^{\Lambda-1} \left(\frac{\pi}{\Lambda}\right)^2 |u(x_{k,l}) - u_h(x_{k,l})|^2 \sin\left(\frac{l\pi}{\Lambda}\right)$$

and

$$\mathcal{E}_4 = \sum_{k=0}^{2\Lambda-1} \sum_{l=0}^{\Lambda-1} \left(\frac{\pi}{\Lambda}\right)^2 |\nabla_{\Gamma} u(x_{k,l}) - \nabla_{\Gamma} u_h(x_{k,l})|^2 \sin\left(\frac{l\pi}{\Lambda}\right).$$

Here,

$$x_{k,l} = \left(\cos\left(\frac{k\pi}{\Lambda}\right) \sin\left(\frac{l\pi}{\Lambda}\right), \sin\left(\frac{k\pi}{\Lambda}\right) \sin\left(\frac{l\pi}{\Lambda}\right), \cos\left(\frac{l\pi}{\Lambda}\right)\right)^T, \quad k = 0, \dots, 2\Lambda - 1, l = 0, \dots, \Lambda - 1$$

and $\Lambda = 200$. We choose f so that $u(x) := (x_1^2 - x_2^2)/|x|^2$ solves (2.3) and set $\varepsilon = 5.333h$. Due to symmetry, we only solve for u_h over D_h in the positive octant, and impose homogenous Neumann boundary conditions for u_h on the boundaries $x_i = 0$, $i = 1, 2, 3$. In Tables 4 – 6 we display the values of \mathcal{E}_i , $i = 1, \dots, 4$, together with the eocs, for $q = 1$, $q = 2$ and $q = 7$ respectively and observe a similar behaviour as in the two-dimensional test example. In Figure 2 we display portions of two of the meshes, $h = 3.750e-02$ (left) and $h = 9.375e-03$ (right), the triangulation $\tilde{\mathcal{T}}_h$ can be identified by the region where the mesh is fine.

Example 3

Here we consider an example similar to the example in Section 9.2 of [15]. We set $\Omega = (-2, 2)^3$ and take Γ to be the zero level surface of

$$\begin{aligned} \phi(x) &= (x_1^2 - 1)^2 + (x_2^2 - 1)^2 + (x_3^2 - 1)^2 + (x_1^2 + x_2^2 - 3)^2 \\ &\quad + (x_1^2 + x_3^2 - 3)^2 + (x_2^2 + x_3^2 - 3)^2 - 10. \end{aligned}$$

We set $f(x) = 10000 \sin(5(x_1 + x_2 + x_3) + 2.5)$ and take $h = 2.2097e-02$, $\varepsilon = 0.2$ as well as $q = 1$. In Figure 3 we display the approximate solution u_h plotted on the zero level surface of $I_h \phi$ together with a cross section of the mesh \mathcal{T}_h . To compute the closet point projection \hat{p} we used a gradient-descent-like iteration from [29].

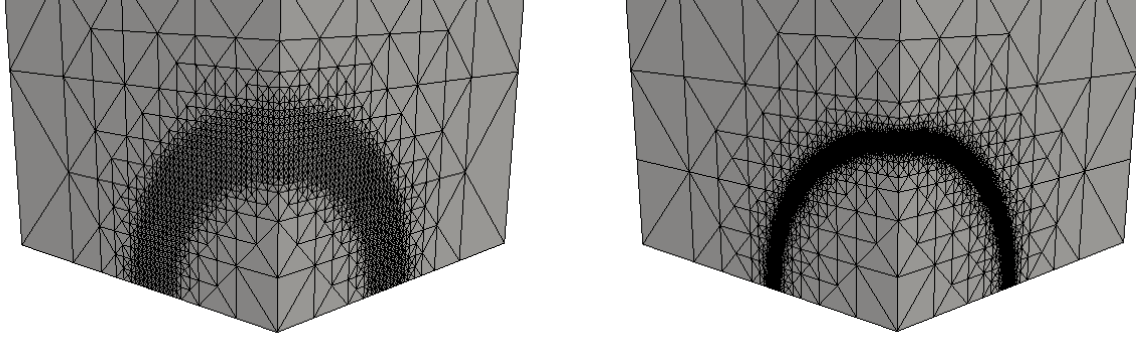


Figure 2: Portions of two of the meshes from Example 2, $h = 3.750e-02$ (left) and $h = 9.375e-03$ (right).

| h | ε | \mathcal{E}_1 | eoc_1 | \mathcal{E}_2 | eoc_2 | \mathcal{E}_3 | eoc_3 | \mathcal{E}_4 | eoc_4 |
|-----------|---------------|-----------------|---------|-----------------|---------|-----------------|---------|-----------------|---------|
| 7.500e-02 | 0.4 | 3.425e-05 | - | 5.504e-03 | - | 8.673e-07 | - | 1.978e-03 | - |
| 3.750e-02 | 0.2 | 6.020e-07 | 5.83 | 5.125e-04 | 3.43 | 1.230e-07 | 2.82 | 4.985e-04 | 1.99 |
| 1.875e-02 | 0.1 | 1.274e-08 | 5.56 | 8.141e-05 | 2.65 | 9.393e-09 | 3.71 | 1.311e-04 | 1.93 |
| 9.375e-03 | 0.05 | 3.729e-10 | 5.09 | 2.361e-05 | 1.79 | 5.447e-10 | 4.11 | 3.214e-05 | 2.03 |

Table 4: Example 2, errors and experimental orders of convergence, $q = 1$.

| h | ε | \mathcal{E}_1 | eoc_1 | \mathcal{E}_2 | eoc_2 | \mathcal{E}_3 | eoc_3 | \mathcal{E}_4 | eoc_4 |
|-----------|---------------|-----------------|---------|-----------------|---------|-----------------|---------|-----------------|---------|
| 7.500e-02 | 0.4 | 1.134e-05 | - | 2.816e-03 | - | 8.523e-07 | - | 2.018e-03 | - |
| 3.750e-02 | 0.2 | 2.082e-07 | 5.77 | 3.146e-04 | 3.16 | 8.472e-08 | 3.33 | 5.002e-04 | 2.01 |
| 1.875e-02 | 0.1 | 5.008e-09 | 5.38 | 5.632e-05 | 2.48 | 6.124e-09 | 3.79 | 1.309e-04 | 1.93 |
| 9.375e-03 | 0.05 | 1.832e-10 | 4.77 | 1.471e-05 | 1.94 | 3.733e-10 | 4.04 | 3.204e-05 | 2.03 |

Table 5: Example 2, errors and experimental orders of convergence, $q = 2$.

| h | ε | \mathcal{E}_1 | eoc_1 | \mathcal{E}_2 | eoc_2 | \mathcal{E}_3 | eoc_3 | \mathcal{E}_4 | eoc_4 |
|-----------|---------------|-----------------|---------|-----------------|---------|-----------------|---------|-----------------|---------|
| 7.500e-02 | 0.4 | 8.438e-07 | - | 7.103e-04 | - | 1.483e-06 | - | 2.085e-03 | - |
| 3.750e-02 | 0.2 | 3.053e-08 | 4.79 | 1.312e-04 | 2.44 | 9.449e-08 | 3.97 | 5.035e-04 | 2.05 |
| 1.875e-02 | 0.1 | 1.557e-09 | 4.29 | 2.993e-05 | 2.13 | 6.253e-09 | 3.92 | 1.308e-04 | 1.94 |
| 9.375e-03 | 0.05 | 9.184e-11 | 4.08 | 7.302e-06 | 2.04 | 3.819e-10 | 4.03 | 3.195e-05 | 2.03 |

Table 6: Example 2, errors and experimental orders of convergence, $q = 7$.

4.1 Results using piecewise quadratic finite elements

Even though we have restricted our error analysis to the case of piecewise linear finite elements it is not difficult to apply our approach to quadratic elements. In order to do so, we use

$$\tilde{V}_h := \left\{ v_h \in C^0(D_h) : v_h \text{ is quadratic on } T \text{ for all } T \in \tilde{\mathcal{T}}_h \right\} \quad (4.1)$$

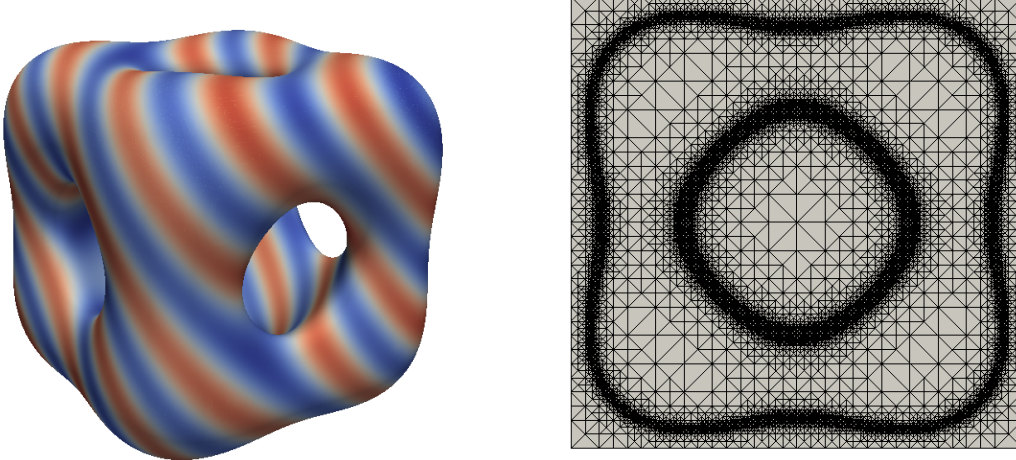


Figure 3: Computational results from Example 3: u_h plotted on the zero level surface of $I_h\phi$, colouring ranges from the minimum -86.45 to the maximum 99.57 of the solution (left), cross section of the mesh \mathcal{T}_h (right).

instead of (2.31) and define the forms a_h and l_h (for the case $a_{ij} = \delta_{ij}, a_0 = 1$) by

$$\begin{aligned}
 a_h(v_1, v_2) &:= \varepsilon^{-1} \sum_{T \in \tilde{\mathcal{T}}_h} Q_T [\varrho \nabla v_{1|T} \cdot \nabla v_{2|T} |\nabla I_h \phi|_T + \varrho v_1 v_2 |\nabla I_h \phi|_T] \\
 l_h(v) &:= \varepsilon^{-1} \sum_{T \in \tilde{\mathcal{T}}_h} Q_T [\varrho I_h \hat{f} v |\nabla I_h \phi|_T],
 \end{aligned}$$

where I_h denotes the Lagrange interpolation operator for piecewise quadratic finite elements. The results in Table 7 correspond to the setting outlined in Example 1. Using a quadrature rule that is exact up to order $q = 7$ we see eocs close to order four for \mathcal{E}_2 and \mathcal{E}_4 in contrast to the eocs close to order two, that are displayed in Table 3, for the corresponding affine finite element approximation. The fact that the eocs for \mathcal{E}_1 and \mathcal{E}_3 are close to four (rather than six as expected for quadratic elements) is a consequence of the term ε^2 in (2.37) which now dominates.

| h | ε | \mathcal{E}_1 | eoc_1 | \mathcal{E}_2 | eoc_2 | \mathcal{E}_3 | eoc_3 | \mathcal{E}_4 | eoc_4 |
|-----------|---------------|-----------------|---------|-----------------|---------|-----------------|---------|-----------------|---------|
| 1.875e-02 | 0.2 | 1.734e-06 | - | 5.016e-05 | - | 5.509e-06 | - | 3.473e-08 | - |
| 9.375e-03 | 0.1 | 1.074e-07 | 4.01 | 3.114e-06 | 4.01 | 3.464e-07 | 3.99 | 1.897e-09 | 4.19 |
| 4.687e-03 | 0.05 | 6.696e-09 | 4.00 | 1.943e-07 | 4.00 | 2.168e-08 | 4.00 | 1.278e-10 | 3.89 |
| 2.344e-03 | 0.025 | 4.183e-10 | 4.00 | 1.214e-08 | 4.00 | 1.356e-09 | 4.00 | 7.641e-12 | 4.06 |
| 1.172e-03 | 0.0125 | 2.614e-11 | 4.00 | 7.588e-10 | 4.00 | 8.473e-11 | 4.00 | 4.781e-13 | 4.00 |

Table 7: Errors and experimental orders of convergence for Example 1, using (4.1) with $q = 7$.

Acknowledgements

VS would like to thank the Isaac Newton Institute for Mathematical Sciences for support and hospitality during the programme *Geometry, compatibility and structure preservation in computational differential equations* when work on this paper was undertaken. This work was supported by: EPSRC grant number EP/R014604/1.

A Appendix

The aim of this appendix is to derive certain properties of the projection p and the extension $u^e(x) = u(p(x))$ which have been used in the analysis above. To begin, we infer from the definition of u^e for $1 \leq i, j \leq n+1$ that

$$u_{x_i}^e(x) = \sum_{k=1}^{n+1} \underline{D}_k u(p(x)) p_{k,x_i}(x); \quad (\text{A.1})$$

$$u_{x_i x_j}^e(x) = \sum_{k,l=1}^{n+1} \underline{D}_l \underline{D}_k u(p(x)) p_{k,x_i}(x) p_{l,x_j}(x) + \sum_{k=1}^{n+1} \underline{D}_k u(p(x)) p_{k,x_i x_j}(x). \quad (\text{A.2})$$

LEMMA. A.1. *Let $k \in \{0, 1, 2\}$ and $u \in H^k(\Gamma)$. Then*

$$|u^e|_{k, U_r} \leq C \sqrt{r} \|u\|_{k, \Gamma}, \quad 0 < r < \delta. \quad (\text{A.3})$$

Proof. Using the transformation $F : \Gamma \times (-r, r) \rightarrow U_r$ with Jacobian determinant μ , (A.1), (A.2) and the fact that $p \in C^2$ we obtain

$$|u^e|_{k, U_r}^2 = \sum_{|\beta|=k} \int_{U_r} |D^\beta u^e(x)|^2 dx \leq C \sum_{|\kappa|=0}^{|\beta|} \int_{-r}^r \int_{\Gamma} |D_\Gamma^\kappa u(p)|^2 \mu(p, s) dS_p ds \leq C r \|u\|_{k, \Gamma}^2$$

and the result follows. \square

In order to obtain more precise information about p and its derivatives we essentially follow the argument in [9, Section 2.1], where the corresponding formulae were derived for the case $A = I$. For $x \in U_\delta$, we consider the function

$$\eta_x(\tau) := F(p(x), (1-\tau)\phi(x)) = \gamma_{p(x)}((1-\tau)\phi(x)), \quad \tau \in [0, 1],$$

where γ_p was defined in (2.11). Since $p \in C^2$, it follows that $(x, \tau) \mapsto \eta_x(\tau)$ has continuous partial derivatives of second order with respect to x . Clearly, $\eta_x(1) = F(p(x), 0) = p(x)$, $\eta_x(0) = F(p(x), \phi(x)) = x$. Furthermore, we infer from (2.11) that for $k = 1, \dots, n+1$

$$\eta'_{x,k}(\tau) = -\phi(x) \gamma'_{p(x),k}((1-\tau)\phi(x)) = -\phi(x) \frac{1}{z_x(\tau)} \sum_{l=1}^{n+1} a_{kl}(p(x)) \phi_{x_l}(\eta_x(\tau)), \quad (\text{A.4})$$

where $z_x(\tau) = \sum_{r,s=1}^{n+1} a_{rs}(p(x)) \phi_{x_r}(\eta_x(\tau)) \phi_{x_s}(\eta_x(\tau))$. Let us abbreviate $w(x) := z_x(0)$. The following relations will help to simplify some of the subsequent calculations.

LEMMA. A.2. *There exist $d_k^A, d^w \in C^2$ such that*

$$\sum_{l=1}^{n+1} a_{kl}(p(x)) \phi_{x_l}(x) = \phi_{x_k}(x) + \phi(x) d_k^A(x), \quad (\text{A.5})$$

$$w(x) = |\nabla \phi(x)|^2 + \phi(x) d^w(x). \quad (\text{A.6})$$

Furthermore, if $f : \Gamma \rightarrow \mathbb{R}$ is differentiable, then there are $d_k^f \in C^2$ such that

$$\sum_{k=1}^{n+1} \underline{D}_k f(p(x)) \phi_{x_k}(x) = \phi(x) \sum_{k=1}^{n+1} \underline{D}_k f(p(x)) d_k^f(x). \quad (\text{A.7})$$

Proof. Recalling that $A(p)\nu(p) = \nu(p)$, $p \in \Gamma$ as well as $\eta_x(0) = x, \eta_x(1) = p(x)$ we obtain with the help of (A.4)

$$\begin{aligned} \sum_{l=1}^{n+1} a_{kl}(p(x))\phi_{x_l}(x) &= \phi_{x_k}(p(x)) + \sum_{l=1}^{n+1} a_{kl}(p(x))(\phi_{x_l}(x) - \phi_{x_l}(p(x))) \\ &= \phi_{x_k}(x) - \sum_{l=1}^{n+1} (a_{kl}(p(x)) - \delta_{kl})(\phi_{x_l}(\eta_x(1)) - \phi_{x_l}(\eta_x(0))) \\ &= \phi_{x_k}(x) + \phi(x)d_k^A(x). \end{aligned} \quad (\text{A.8})$$

Note that $d_k^A \in C^2$, since this is true for $x \mapsto \eta_x$ and $x \mapsto a_{kl}(p(x))$. The relation (A.6) immediately follows from (A.5). Next, observing that $\nabla_\Gamma f(p(x)) \in T_{p(x)}\Gamma$ and $\nabla\phi(p(x)) \perp T_{p(x)}\Gamma$ we infer that

$$\sum_{k=1}^{n+1} \underline{D}_k f(p(x)) \phi_{x_k}(x) = \sum_{k=1}^{n+1} \underline{D}_k f(p(x)) (\phi_{x_k}(x) - \phi_{x_k}(p(x))),$$

which implies (A.7) in a similar way as above. \square

Inserting (A.5) and (A.6) into (A.4) we infer that there exist $d_k^{\eta,1} \in C^2$ such that

$$\eta'_{x,k}(0) = -\frac{\phi(x)\phi_{x_k}(x)}{|\nabla\phi(x)|^2} + \phi(x)^2 d_k^{\eta,1}(x), \quad 1 \leq k \leq n+1. \quad (\text{A.9})$$

If we differentiate (A.4) and use again (A.4) we obtain

$$\begin{aligned} \eta''_{x,k}(\tau) &= -\frac{\phi(x)}{z_x(\tau)} \sum_{l,m=1}^{n+1} a_{kl}(p(x))\phi_{x_l x_m}(\eta_x(\tau))\eta'_{x,m}(\tau) + \frac{\phi(x)}{z_x(\tau)^2} z'_x(\tau) \sum_{l=1}^{n+1} a_{kl}(p(x))\phi_{x_l}(\eta_x(\tau)) \\ &= \frac{\phi(x)^2}{z_x(\tau)^2} \sum_{l,m,q=1}^{n+1} a_{kl}(p(x))a_{mq}(p(x))\phi_{x_l x_m}(\eta_x(\tau))\phi_{x_q}(\eta_x(\tau)) \\ &\quad - 2\frac{\phi(x)^2}{z_x(\tau)^2} \sum_{l,m,q,r,s=1}^{n+1} a_{kl}(p(x))a_{mq}(p(x))a_{rs}(p(x))\phi_{x_r x_m}(\eta_x(\tau))\phi_{x_l}(\eta_x(\tau))\phi_{x_q}(\eta_x(\tau))\phi_{x_s}(\eta_x(\tau)). \end{aligned} \quad (\text{A.10})$$

Taylor's theorem together with (A.9) and (A.10) implies the existence of $d_k^{p,0} \in C^2$ with

$$\begin{aligned} p_k(x) &= \eta_{x,k}(1) = \eta_{x,k}(0) + \eta'_{x,k}(0) + \int_0^1 (1-\tau)\eta''_{x,k}(\tau)d\tau \\ &= x_k - \frac{\phi(x)\phi_{x_k}(x)}{|\nabla\phi(x)|^2} + \phi(x)^2 d_k^{p,0}(x). \end{aligned} \quad (\text{A.11})$$

The relation (A.11) allows us to prove a bound between $p(x)$ and the closest-point projection $\hat{p}(x)$, which is used in the error analysis.

LEMMA. A.3. *There exists a constant C such that*

$$|p(x) - \hat{p}(x)| \leq C \phi(x)^2 \quad \forall x \in U_\delta. \quad (\text{A.12})$$

Proof. Let us fix $x \in U_\delta$. Using (A.11) and the fact that $p(x) \in \Gamma$ we have

$$|x - \widehat{p}(x)| \leq |x - p(x)| \leq C|\phi(x)|.$$

Furthermore, since $T_{\widehat{p}(x)}\Gamma = \text{span}\{\nabla\phi(\widehat{p}(x))\}^\perp$, (2.1) implies that there exists $\lambda \in \mathbb{R}$ such that $x - \widehat{p}(x) = \lambda \nabla\phi(\widehat{p}(x))$. Taylor expansion around $\widehat{p}(x)$ yields together with $\phi(\widehat{p}(x)) = 0$, that

$$\begin{aligned} \phi(x) &= \nabla\phi(\widehat{p}(x)) \cdot (x - \widehat{p}(x)) + \frac{1}{2}(x - \widehat{p}(x))^t D^2\phi(\xi)(x - \widehat{p}(x)) \\ &= \lambda |\nabla\phi(\widehat{p}(x))|^2 + \frac{1}{2}(x - \widehat{p}(x))^t D^2\phi(\xi)(x - \widehat{p}(x)) \end{aligned}$$

for some $\xi \in [\widehat{p}(x), x]$. Thus

$$\lambda = \frac{\phi(x)}{|\nabla\phi(\widehat{p}(x))|^2} + r, \quad \text{where } |r| \leq C|x - \widehat{p}(x)|^2 \leq C\phi(x)^2$$

and therefore

$$x - \widehat{p}(x) = \phi(x) \frac{\nabla\phi(\widehat{p}(x))}{|\nabla\phi(\widehat{p}(x))|^2} + r \nabla\phi(\widehat{p}(x)). \quad (\text{A.13})$$

If we combine this relation with (A.11) we find that

$$p(x) - \widehat{p}(x) = \phi(x) \left[\frac{\nabla\phi(\widehat{p}(x))}{|\nabla\phi(\widehat{p}(x))|^2} - \frac{\nabla\phi(x)}{|\nabla\phi(x)|^2} \right] + r \nabla\phi(\widehat{p}(x)) + \phi(x)^2 d^{p,0}(x),$$

from which we deduce (A.12), since $|x - \widehat{p}(x)| \leq C|\phi(x)|$ and $|r| \leq C\phi(x)^2$. \square

Our next aim is to improve on (A.11) by using a Taylor expansion of one degree higher. We deduce from (A.10), (A.5) and (A.6) that

$$\begin{aligned} \eta''_{x,k}(0) &= \frac{\phi(x)^2}{w(x)^2} \sum_{l,m,q=1}^{n+1} a_{kl}(p(x)) a_{mq}(p(x)) \phi_{x_l x_m}(x) \phi_{x_q}(x) \\ &\quad - 2 \frac{\phi(x)^2}{w(x)^2} \sum_{l,m,q,r,s=1}^{n+1} a_{kl}(p(x)) a_{mq}(p(x)) a_{rs}(p(x)) \phi_{x_r x_m}(x) \phi_{x_l}(x) \phi_{x_q}(x) \phi_{x_s}(x) \\ &= \frac{\phi(x)^2}{|\nabla\phi(x)|^4} \sum_{l,m=1}^{n+1} a_{kl}(p(x)) \phi_{x_l x_m}(x) \phi_{x_m}(x) \\ &\quad - 2 \frac{\phi(x)^2 \phi_{x_k}(x)}{|\nabla\phi(x)|^4} \sum_{m,r=1}^{n+1} \phi_{x_r}(x) \phi_{x_m}(x) \phi_{x_r x_m}(x) + \phi(x)^3 d_k^{\eta,2}(x), \end{aligned} \quad (\text{A.14})$$

where $d_k^{\eta,2} \in C^2$. Differentiating (A.10) and using (A.4) as well as (A.14) we obtain

$$\begin{aligned} p_k(x) &= \eta_{x,k}(1) = \eta_{x,k}(0) + \eta'_{x,k}(0) + \frac{1}{2} \eta''_{x,k}(0) + \frac{1}{2} \int_0^1 (1-\tau)^2 \eta'''_{x,k}(\tau) d\tau \\ &= x_k - \frac{\phi(x)}{w(x)} \sum_{l=1}^{n+1} a_{kl}(p(x)) \phi_{x_l}(x) + \frac{1}{2} \frac{\phi(x)^2}{|\nabla\phi(x)|^4} \sum_{l,m=1}^{m+1} a_{kl}(p(x)) \phi_{x_l x_m}(x) \phi_{x_m}(x) \\ &\quad - \frac{\phi(x)^2 \phi_{x_k}(x)}{|\nabla\phi(x)|^4} \sum_{m,r=1}^{n+1} \phi_{x_r}(x) \phi_{x_m}(x) \phi_{x_r x_m}(x) + \phi(x)^3 \tilde{d}_k^{p,0}(x), \end{aligned} \quad (\text{A.15})$$

where $\tilde{d}_k^{p,0} \in C^2$.

Before we continue let us remark that we may deduce from (A.11)

$$p_{k,x_i}(x) = \delta_{ik} - \frac{\phi_{x_i}(x)\phi_{x_k}(x)}{|\nabla\phi(x)|^2} + \phi(x)d_{ik}^{p,1}(x), \quad 1 \leq i, k \leq n+1, \quad (\text{A.16})$$

where $d_{ik}^{p,1} \in C^1$. Combining this relation with (A.7) we obtain

$$\begin{aligned} \frac{\partial}{\partial x_i} [a_{kl}(p(x))] &= \sum_{m=1}^{n+1} \underline{D}_m a_{kl}(p(x)) p_{m,x_i}(x) \\ &= \underline{D}_i a_{kl}(p(x)) - \sum_{m=1}^{n+1} \underline{D}_m a_{kl}(p(x)) \frac{\phi_{x_i}(x)\phi_{x_m}(x)}{|\nabla\phi(x)|^2} + \phi(x) \sum_{m=1}^{n+1} \underline{D}_m a_{kl}(p(x)) d_{im}^{p,1}(x) \\ &= \underline{D}_i a_{kl}(p(x)) + \phi(x) d_{kl}^{A,i}(x), \end{aligned} \quad (\text{A.17})$$

where $d_{kl}^{A,i} \in C^1$. Differentiating (A.15) with respect to x_i and using (A.17), (A.6) we deduce for $1 \leq i, k \leq n+1$

$$\begin{aligned} p_{k,x_i}(x) &= \delta_{ik} - \frac{\phi_{x_i}(x)}{w(x)} \sum_{l=1}^{n+1} a_{kl}(p(x)) \phi_{x_l}(x) + \phi(x) \frac{\phi_{x_k}(x) w_{x_i}(x)}{|\nabla\phi(x)|^4} - \phi(x) \sum_{l=1}^{n+1} \frac{\underline{D}_l a_{kl}(p(x)) \phi_{x_l}(x)}{|\nabla\phi(x)|^2} \\ &\quad - \phi(x) \sum_{l=1}^{n+1} \frac{a_{kl}(p(x)) \phi_{x_l x_i}(x)}{|\nabla\phi(x)|^2} + \frac{\phi(x) \phi_{x_i}(x)}{|\nabla\phi(x)|^4} \sum_{l,m=1}^{m+1} a_{kl}(p(x)) \phi_{x_l x_m}(x) \phi_{x_m}(x) \\ &\quad - 2 \frac{\phi(x) \phi_{x_i}(x) \phi_{x_k}(x)}{|\nabla\phi(x)|^4} \sum_{m,r=1}^{n+1} \phi_{x_r}(x) \phi_{x_m}(x) \phi_{x_r x_m}(x) + \phi(x)^2 \tilde{d}_{ik}^{p,1}(x), \end{aligned} \quad (\text{A.18})$$

where $\tilde{d}_{ik}^{p,1} \in C^1$. If we differentiate this relation with respect to x_j and use (A.5), (A.17) we infer for $1 \leq i, j, k \leq n+1$

$$\begin{aligned} p_{k,x_i x_j}(x) &= - \sum_{l=1}^{n+1} \left\{ \frac{\underline{D}_j a_{kl}(p(x)) \phi_{x_i}(x) \phi_{x_l}(x)}{|\nabla\phi(x)|^2} + \frac{\underline{D}_i a_{kl}(p(x)) \phi_{x_j}(x) \phi_{x_l}(x)}{|\nabla\phi(x)|^2} \right\} \\ &\quad - \sum_{l=1}^{n+1} \left\{ \frac{a_{kl}(p(x)) \phi_{x_i}(x) \phi_{x_l x_j}(x)}{|\nabla\phi(x)|^2} + \frac{a_{kl}(p(x)) \phi_{x_j}(x) \phi_{x_l x_i}(x)}{|\nabla\phi(x)|^2} \right\} \\ &\quad + \sum_{l,m=1}^{n+1} \frac{a_{kl}(p(x)) \phi_{x_i}(x) \phi_{x_j}(x) \phi_{x_m}(x) \phi_{x_l x_m}(x)}{|\nabla\phi(x)|^4} \\ &\quad + \beta_{ijk}(x) \phi_{x_k}(x) + \phi(x) \tilde{d}_{ijk}^{p,2}(x) + \phi(x)^2 \tilde{d}_{ijk}^{p,3}(x), \end{aligned} \quad (\text{A.19})$$

where $\beta_{ijk}, \tilde{d}_{ij}^{p,2} \in C^1, \tilde{d}_{ijk}^{p,3} \in C^0$. Using the above formulae we now obtain:

LEMMA. A.4. *Suppose that $u : \Gamma \rightarrow \mathbb{R}$ is a solution of (2.3). Then, u^e satisfies (2.16), (2.17).*

Proof. Combining (A.1), (A.16) and (A.7) we deduce that

$$u_{x_i}^e(x) = \sum_{k=1}^{n+1} \underline{D}_k u(p(x)) p_{k,x_i}(x) = \underline{D}_i u(p(x)) + \phi(x) \sum_{k=1}^{n+1} \alpha_k^i(x) \underline{D}_k u(p(x)), \quad (\text{A.20})$$

where $\alpha_k^i \in C^1$. Similarly, using (A.2), (A.16), (A.19) and (A.7) we obtain

$$\begin{aligned}
u_{x_i x_j}^e(x) &= \sum_{k,l=1}^{n+1} \underline{D}_l \underline{D}_k u(p(x)) p_{k,x_i}(x) p_{l,x_j}(x) + \sum_{k=1}^{n+1} \underline{D}_k u(p(x)) p_{k,x_i x_j}(x) \\
&= \sum_{k=1}^{n+1} \underline{D}_j \underline{D}_k u(p(x)) \left(\delta_{ik} - \frac{\phi_{x_i}(x) \phi_{x_k}(x)}{|\nabla \phi(x)|^2} \right) \\
&\quad - \sum_{k,l=1}^{n+1} \underline{D}_k u(p(x)) \left\{ \frac{\underline{D}_j a_{kl}(p(x)) \phi_{x_i}(x) \phi_{x_l}(x)}{|\nabla \phi(x)|^2} + \frac{\underline{D}_i a_{kl}(p(x)) \phi_{x_j}(x) \phi_{x_l}(x)}{|\nabla \phi(x)|^2} \right\} \\
&\quad - \sum_{k,l=1}^{n+1} \underline{D}_k u(p(x)) \left\{ \frac{a_{kl}(p(x)) \phi_{x_i}(x) \phi_{x_l x_j}(x)}{|\nabla \phi(x)|^2} + \frac{a_{kl}(p(x)) \phi_{x_j}(x) \phi_{x_l x_i}(x)}{|\nabla \phi(x)|^2} \right\} \\
&\quad + \sum_{k,l,m=1}^{n+1} \underline{D}_k u(p(x)) \frac{a_{kl}(p(x)) \phi_{x_i}(x) \phi_{x_j}(x) \phi_{x_m}(x) \phi_{x_l x_m}(x)}{|\nabla \phi(x)|^4} \\
&\quad + \sum_{1 \leq |\kappa| \leq 2} (\phi(x) \alpha_\kappa^{ij}(x) + \phi(x)^2 \tilde{\alpha}_\kappa^{ij}(x)) D_\Gamma^\kappa u(p(x)), \tag{A.21}
\end{aligned}$$

where $\alpha_\kappa^{ij} \in C^1$, $\tilde{\alpha}_\kappa^{ij} \in C^0$. Recalling (A.5) and using (A.21) and the symmetry of the coefficients a_{ij} we infer that

$$\begin{aligned}
\sum_{i,j=1}^{n+1} a_{ij}^e(x) u_{x_i x_j}^e(x) &= \sum_{i,j=1}^{n+1} a_{ij}(p(x)) u_{x_i x_j}^e(x) \\
&= \sum_{i,j=1}^{n+1} a_{ij}(p(x)) \underline{D}_j \underline{D}_i u(p(x)) - \sum_{j,k=1}^{n+1} \underline{D}_j \underline{D}_k u(p(x)) \frac{\phi_{x_j}(x) \phi_{x_k}(x)}{|\nabla \phi(x)|^2} \\
&\quad - 2 \sum_{j,k,l=1}^{n+1} \underline{D}_k u(p(x)) \underline{D}_j a_{kl}(p(x)) \frac{\phi_{x_j}(x) \phi_{x_l}(x)}{|\nabla \phi(x)|^2} - \sum_{k,l,m=1}^{n+1} a_{kl}(p(x)) \underline{D}_k u(p(x)) \frac{\phi_{x_m}(x) \phi_{x_l x_m}(x)}{|\nabla \phi(x)|^2} \\
&\quad + \sum_{1 \leq |\kappa| \leq 2} (\phi(x) \beta_\kappa(x) + \phi(x)^2 \tilde{\beta}_\kappa(x)) D_\Gamma^\kappa u(p(x)) \\
&= \sum_{i,j=1}^{n+1} a_{ij}(p(x)) \underline{D}_j \underline{D}_i u(p(x)) - \sum_{k,l,m=1}^{n+1} a_{kl}(p(x)) \underline{D}_k u(p(x)) \frac{\phi_{x_m}(x) \phi_{x_l x_m}(x)}{|\nabla \phi(x)|^2} \\
&\quad + \sum_{1 \leq |\kappa| \leq 2} (\phi(x) \gamma_\kappa(x) + \phi(x)^2 \tilde{\gamma}_\kappa(x)) D_\Gamma^\kappa u(p(x)), \tag{A.22}
\end{aligned}$$

where the last identity follows from (A.7) and where $\gamma_\kappa \in C^1$, $\tilde{\gamma}_\kappa \in C^0$. On the other hand, (A.17) and (A.20) yield

$$\sum_{i,j=1}^{n+1} a_{ij,x_j}^e(x) u_{x_i}^e(x) = \sum_{i,j=1}^{n+1} \underline{D}_j a_{ij}(p(x)) \underline{D}_i u(p(x)) + \phi(x) \sum_{k=1}^{n+1} \tilde{\beta}_k(x) \underline{D}_k u(p(x)), \tag{A.23}$$

where $\tilde{\beta}_k \in C^1$. Combining (A.22) and (A.23) we find that

$$\frac{1}{|\nabla \phi(x)|} \nabla \cdot (A^e(x) \nabla u^e(x) |\nabla \phi(x)|)$$

$$\begin{aligned}
&= \sum_{i,j=1}^{n+1} (a_{ij,x_j}^e(x)u_{x_i}^e(x) + a_{ij}^e(x)u_{x_i x_j}^e(x)) + \frac{1}{|\nabla\phi(x)|^2} \sum_{i,j,k=1}^{n+1} a_{ij}^e(x)u_{x_i}^e(x)\phi_{x_k}(x)\phi_{x_k x_j}(x) \\
&= \sum_{i,j=1}^{n+1} \underline{D}_j(a_{ij}(p(x))\underline{D}_i u(p(x))) + \sum_{1 \leq |\kappa| \leq 2} (\phi(x)b_\kappa(x) + \phi(x)^2 c_\kappa(x)) D_\Gamma^\kappa u(p(x)),
\end{aligned}$$

where $b_\kappa \in C^1, c_\kappa \in C^0$. Combining this relation with (2.3) implies (2.16) and (2.17). \square

References

- [1] Barrett, J.W and Nürnberg, R. and Styles, V.: *Finite element approximation of a phase field model for void electromigration*. SIAM J. Numer. Anal. **46**, 738–772 (2004).
- [2] Bertalmio, M., Cheng, L.T., Osher, S., Sapiro, G.: *Variational problems and partial differential equations on implicit surfaces: The framework and examples in image processing and pattern formation*. J. Comput. Phys. **174**, 759–780 (2001).
- [3] Bonito, A., Demlow, A., Nchetto, R.H.: *Finite element methods for the Laplace-Beltrami operator*. Handbook of Numerical Analysis, vol. XXI, Geometric Partial Differential Equations - Part 1 (2020).
- [4] Burger, M: *Finite element approximation of elliptic partial differential equations on implicit surfaces*. Comput. Vis. Sci. **12**, 87–100 (2009).
- [5] Burman, E., Hansbo, P., Larson, M.G.: *A stabilized cut finite element method for partial differential equations on surfaces: The Laplace–Beltrami operator*. Comput. Methods Appl. Mech. Engrg. **285**, 188-207 (2015).
- [6] Burman, E., Hansbo, P., Larson, M.G., Massing, A., Zahedi, S.: *Full gradient stabilized cut finite element methods for surface partial differential equations*. Comput. Methods Appl. Mech. Engrg. **310**, 278-296 (2016).
- [7] Chernyshenko, A.Y, Olshanskii, M.A.: *Non-degenerate Eulerian finite element method for solving PDEs on surfaces*. Russian J. Numer. Anal. Math. Modelling **28**, no. 2, 101-124 (2013).
- [8] Deckelnick, K., Dziuk, G., Elliott, C.M., Heine, C.-J.: *An h-narrow band finite-element method for elliptic equations on implicit surfaces*. IMA J. Numer. Anal. **30**, 351–376 (2010).
- [9] Deckelnick, K., Elliott, C.M., Ranner, T.: *Unfitted finite element methods using bulk meshes for surface partial differential equations*. SIAM J. Numer. Anal. **52**, 2137–2162 (2014).
- [10] Deckelnick, K., Styles, V.: *Stability and error analysis for a diffuse interface approach to an advection-diffusion equation on a moving surface*. Numer. Math. **139**, 709–741 (2018).
- [11] Demlow, A.: *Higher-order finite element methods and pointwise error estimates for elliptic problems on surfaces*. SIAM J. Numer. Anal. **47**, no. 2, 805-827 (2009).
- [12] Demlow, A., Dziuk, G.: *An adaptive finite element method for the Laplace–Beltrami operator on implicitly defined surfaces*. SIAM J. Numer. Anal. **45**, 421–442 (2007).

- [13] Demlow, A., Olshanskii, M.A.: *An adaptive surface finite element method based on volume meshes*. SIAM J. Numer. Anal. **50**, no. 3, 1624-1647 (2012).
- [14] Dziuk, G.: *Finite elements for the Beltrami operator on arbitrary surfaces*. In: Partial differential equations and calculus of variations, S. Hildebrandt and R. Leis, eds., vol. 1357 of Lecture Notes in Mathematics, Springer-Verlag, Berlin, 1988, pp. 142–155.
- [15] Dziuk, G., Elliott, C.M.: *Finite element methods for surface PDEs*. Acta Numer. **22**, 289–396 (2013).
- [16] Elliott, C.M., Stinner, B.: *Analysis of a diffuse interface approach to an advection diffusion equation on a moving surface*. Math. Models Methods Appl. Sci. **19**, 787–802 (2009).
- [17] Elliott, C.M., Stinner, B., Styles, V., Welford, R.: *Numerical computation of advection and diffusion on evolving diffuse interfaces*. IMA J. Numer. Anal. **31**, 786–812 (2011).
- [18] Elliott, C.M., Ranner, T.: *Finite element analysis for a coupled bulk–surface partial differential equation*. IMA J. Numer. Anal. **33**, 377–402 (2013).
- [19] Gilbarg, D., Trudinger, N.S.: *Elliptic Partial Differential Equations of Second Order*, Springer-Verlag, Berlin, 2nd ed., 1988.
- [20] Grande, J., Lehrenfeld, C., Reusken, A.: *Analysis of a high-order trace finite element method for PDEs on level set surfaces*. SIAM J. Numer. Anal. **56**, 228–255 (2018).
- [21] Hansbo, A., Hansbo, P.: *An unfitted finite element method, based on Nitsche’s method, for elliptic interface problems*. Comput. Methods Appl. Mech. Engrg. **191**, 5537–5552 (2002).
- [22] Hansbo, A., Hansbo, P.: *A finite element method for the simulation of strong and weak discontinuities in solid mechanics*. Comput. Methods Appl. Mech. Engrg. **193**, 3523–3540 (2004).
- [23] Macdonald, C.B., Ruuth, S.J.: *The Implicit Closest Point Method for the Numerical Solution of Partial Differential Equations on Surfaces*. SIAM J. Sci. Comput. **31**, 4330-4350 (2009).
- [24] Olshanskii, M.A., Reusken, A.: *A finite element method for surface PDEs: matrix properties*. Numer. Math. **114**, no. 3, 491-520 (2010).
- [25] Olshanskii, M.A., Reusken, A., Grande, J.: *A finite element method for elliptic equations on surfaces*. SIAM J. Numer. Anal. **47**, no. 5, 3339-3358 (2009).
- [26] Olshanskii, M.A., Safin, D.: *A narrow-band unfitted finite element method for elliptic PDEs posed on surfaces*. Math. Comp. **85**, no. 300, 1549–1570 (2016).
- [27] Rätz, A., Voigt, A.: *PDE’s on surfaces - a diffuse interface approach*. Comm. Math. Sci. **4**, 575–590 (2006).
- [28] Reusken, A.: *Analysis of trace finite element methods for surface partial differential equations*. IMA J. Numer. Anal. **35**, no. 4, 1568–1590 (2015).
- [29] Reusken, A.: *A finite element level set redistancing method based on gradient recovery*. SIAM J. Numer. Anal. **51** 2723–2745 (2013).

- [30] Schmidt, A. and Siebert, K.G.: *Design of adaptive finite element software. The finite element toolbox ALBERTA*. Lecture Notes in Computational Science and Engineering 42, Springer-Verlag, Berlin, (2005).